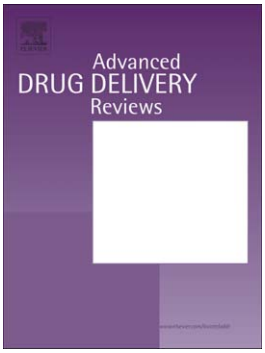

Polymorphic Phase Transitions: Macroscopic Theory and Molecular Simulation

Jamshed Anwar, Dirk Zahn

PII: S0169-409X(17)30198-9
DOI: doi:10.1016/j.addr.2017.09.017
Reference: ADR 13187

To appear in: *Advanced Drug Delivery Reviews*

Received date: 2 June 2017
Revised date: 27 August 2017
Accepted date: 7 September 2017

Please cite this article as: Jamshed Anwar, Dirk Zahn, Polymorphic Phase Transitions: Macroscopic Theory and Molecular Simulation, *Advanced Drug Delivery Reviews* (2017), doi:10.1016/j.addr.2017.09.017

Polymorphic Phase Transitions: Macroscopic Theory and Molecular Simulation

Jamshed Anwar[a,*], Dirk Zahn[b,*]

[a] *Chemical Theory and Computation, Department of Chemistry, Lancaster University, Lancaster LA1 4YB, United Kingdom*

[b] *Lehrstuhl für Theoretische Chemie / Computer-Chemie-Centrum, Friedrich-Alexander-Universität Erlangen-Nürnberg, Nägelsbachstr. 25, 91052 Erlangen, Germany*

*Corresponding Authors: j.anwar@lancaster.ac.uk, dirk.zahn@fau.de

Abstract

Transformations in the solid state are of considerable interest, both for fundamental reasons and because they underpin important technological applications. The interest spans a wide spectrum of disciplines and application domains. For pharmaceuticals, a common issue is unexpected polymorphic transformation of the drug or excipient during processing or on storage, which can result in product failure. A more ambitious goal is that of exploiting the advantages of metastable polymorphs (e.g. higher solubility and dissolution rate) while ensuring their stability with respect to solid state transformation. To address these issues and to advance technology, there is an urgent need for significant insights that can only come from a detailed molecular level understanding of the involved processes. Whilst experimental approaches at best yield time- and space-averaged structural information, molecular simulation offers unprecedented, time-resolved molecular-level resolution of the processes taking place. This review aims to provide a comprehensive and critical account of state-of-the-art methods for modelling polymorph stability and transitions between solid phases. This is flanked by revisiting the associated macroscopic theoretical framework for phase transitions, including their classification, proposed molecular mechanisms, and kinetics. The simulation methods are presented in tutorial form, focusing on their application to phase transition phenomena. We describe molecular simulation studies for crystal structure prediction and polymorph screening, phase coexistence and phase diagrams, simulations of crystal-crystal transitions of various types (displacive/martensitic, reconstructive and diffusive), effects of defects, and phase stability and transitions at the nanoscale. Our selection of literature is intended to illustrate significant insights, concepts and understanding, as well as the current scope of using molecular simulations for understanding polymorphic transitions in an accessible way, rather than claiming completeness. With exciting prospects in both simulation methods development and enhancements in computer hardware, we are on the verge of accessing an unprecedented capability for designing and developing dosage forms and drug delivery systems in silico, including tackling challenges in polymorph control on a rational basis.

Contents

1 Introduction

Crystal to crystal phase transitions are of considerable scientific interest and industrial importance. The interest spans numerous fields and application domains that include Earth sciences [1,2], materials science [3-5], biomineralisation [6-8], explosives [9], and pharmaceuticals [10,11]. For pharmaceuticals, drug substances and formulation excipients can exist in different solid forms, with particular form(s) having advantages over others in terms of efficacy, ease of manufacture, or stability on storage [12-17]. Such a selected form within a formulation may transform to another on storage or during manufacture with potentially disastrous consequences including loss of efficacy [15-17]. An infamous example is that of the protease inhibitor Norvir® (retonovir) developed for the treatment of HIV-1, for which the second, a previously unobserved polymorph precipitated in the soft gelatin capsule resulting in a product recall [18]. Indeed, the issue is recognised by the major product licensing authorities, whose guidelines recommend that the polymorphism of all new drug entities is thoroughly investigated [19,20].

Phase transitions in crystals of drugs and excipients have been studied extensively [10,11], with the focus being largely on causal factors, characterization of the phases, and to a lesser extent kinetics. However, despite this interest, our understanding of the mechanisms by which such transitions occur and the factors that govern the kinetics is still relatively rudimentary. In particular, we do not have a handle on the molecular level processes occurring during the phase transitions. Experimental approaches at best (e.g. X-ray or neutron diffraction) yield time and space-averaged structural information, which for polymorphic forms implies primarily the coordinates of the starting (parent) and the final (daughter) crystalline form. The molecular processes occurring during nucleation or at the transition interface are generally inaccessible. This lack of molecular level understanding is limiting the development of strategy and rational approaches that could potentially lead to significant technological impact e.g. reliable stabilization of metastable forms that offer benefits such as enhanced bioavailability or ease of processing.

Computer simulation, more precisely, molecular simulation, offers the required molecular resolution to make the critical molecular processes in phase transitions accessible [21-23]. The basis for molecular simulation are the forces between atoms, which are now relatively well

characterized. These forces enable the simulation of the molecular trajectories to yield effectively a molecular-resolution microscope, albeit based on simulation. Molecular simulation is now transforming our understanding of phase transition phenomena as we illustrate below. The simulations promise molecular level insights that will rationalize experimental observations, predict phase stability and transition kinetics, and enable the development of a robust theoretical framework that could drive advances in pharmaceutical technology.

The review is concerned primarily with the understanding of polymorph phase stability and phase transitions in the solid state. The emphasis is on molecular crystals, given that drug molecules are mostly organic. We also, however, refer to simulations on ionic or inorganic systems wherever they offer generic inferences and studies on molecular systems are lacking. In particular, the interest lies in the molecular level processes that characterize how transitions are initiated and propagate. We set out to develop a coherent understanding of polymorph phase stability and phase transitions, including their classification, mechanisms, and kinetics. The literature on phase transitions is vast, disparate, and continually expanding, and insights and developments in one (sub)discipline rarely carry over into another. This is not surprising given that phase transitions in solids are a ubiquitous phenomenon, exhibited by a spectrum of materials. Here we identify and develop unifying concepts with a view to providing a better understanding of the nature of phase transitions. The discussion is focused on first-order phase transitions given their applicability to polymorphic phase transitions.

We should add that whilst we favour the term *phase transition* rather than *phase transformation*, we believe the current consensus assumes the two terms to be synonymous and consequently we employ as such. We do not review the literature in any comprehensive way, but rather use the literature to discuss or highlight molecular insights, or illustrate a particular issue or behavior. Notable reviews or monographs on phase transitions in solids include: the classic text of Christian [24] though focused on metals and alloys; the more general monographs of Rao and Rao [25], Toledano and Dmitriev [26], Mnyukh [27], and Fultz [5]; pharmaceutically-focused review by Morris et. al. [10]; and reviews with an emphasis on transformation mechanisms by Herbstein [28], James and Hane [29] on martensitic transformations, and that by Dove [30] on displacive transitions in minerals. Particularly insightful are the review papers by Ubbelohde [31-35], despite being rather dated.

2 Crystal polymorphism and phase stability

Crystal polymorphism is defined as the ability of a substance, of a constant chemical composition, to exist in more than one crystalline structure. In its broadest definition, the concept includes all possible differences in the crystalline structure with the exception of homogeneous deformation, but excludes solvates and amorphous modifications. Structurally, the different modifications, or polymorphs, differ in the arrangement of the atoms or atomic groups in a space lattice. These differences may be slight, involving only reorientation of identical atomic groups on the same lattice, or total with little or no relationship between either the connectivity of atomic groups (which may have entirely different coordination numbers) or the lattices. Polymorphism is particularly abundant for molecular compounds which, in addition to differences in the packing of the molecules, may also exhibit conformational differences that include different resonance structures and rotation of moieties around a single bond [36].

Polymorphs of a given compound, whilst having identical chemical properties (though they may differ in terms of solid state reactivity) can differ markedly in their physical properties. Properties affected include solubility, melting point, hardness, density, chemical stability, crystal morphology and various optical and electrical characteristics [12,13,15,37, and references in therein]. [Polymorph energy levels of within a few tenths of kJ/mol are anything but rare. Very abundant and very important, critical and relevant to pharma]

The phenomenon of polymorphism is ubiquitous [38] and its importance in pharmaceutical development is well recognised. Use of an appropriate polymorph can enhance the rate and extent of absorption of the drug into the bloodstream, improve the chemical or physical stability of the product, or ease the necessary processing involved in the manufacture of the pharmaceutical product [12,13,15, and references therein].

A significant proportion of problems of product instability occur as a result of polymorphic phase transitions. On storage or processing, the selected polymorph transforms to a more stable form. Examples of problems encountered include reduction in syringeability of injectable products, caking of suspensions, grittiness in creams and ointments (which may cause these products to be not only cosmetically unacceptable but also painful on application), crystal growth in products intended to be solutions, and depression of the melting point of suppositories such

that their use in the summer becomes impractical [12,13,39,40]. The new phase may exhibit a different solubility and hence dissolution kinetics, which in turn may adversely affect the bioavailability. Clearly, to avoid such issues, the appropriate choice of polymorph would be that which is thermodynamically stable under the conditions of storage experienced by the product. However, this is at odds with the often-desired need to increase the solubility of the drug with a view to enhancing its bioavailability, which can be met by a thermodynamically metastable form. Moreover, the conflicting storage versus bioavailability issues may be complicated by processing, for instance it has been demonstrated that the pressures normally employed in tabletting can also induce phase transformations in drugs [41-43], as can milling [44].

Classical thermodynamics provides a general and sound basis for understanding structural phase transformations, such as those exhibited by polymorphic forms. The Clausius-Clapeyron equation, Gibbs phase rule [45] and the Gibbs free energy function G all satisfactorily predict the important features exhibited by such transformations. In thermodynamics, a *spontaneous* reaction is defined as one that has a natural tendency to proceed without the assistance of any external potential, and is therefore feasible. Note, however, that nothing is implied in this definition about the mechanism and any associated energy barriers, and thus the rate at which the reaction proceeds. Spontaneous reactions are characterised by a negative change in the Gibbs free energy function which is given by

$$\Delta G = \Delta U + p\Delta V - T\Delta S \qquad (1)$$

where T is the absolute temperature, S is the entropy, U is the internal energy, p the pressure and V volume.

It follows that under any given set of conditions of temperature and pressure, of the many possible phases, only the one with the lowest value of G will be thermodynamically stable. All other phases, under the same set of conditions, will be unstable and would tend to transform to the stable phase.

The Gibbs free energy surface $G(p,T)$, therefore, provides a convenient means for examining the respective stability of different phases. Such a free energy profile but as a function only of temperature (with pressure fixed at ambient) is shown for a hypothetical dimorphic system in Figure 1. Points of intersection of the G surfaces of the phases represent conditions at which the

phases are in equilibrium with each other and can co-exist. At these points $\Delta G = 0$ for a transition between the phases. The conditions at the intersection points, that is, temperature and pressure, are referred to as the transition conditions, since any departure from them results in one of the phases becoming thermodynamically stable, provoking the transformation of the other phases to this one. For the system in Figure 1 the transition temperature is $T_{I\text{-}II}$. Below this temperature, Form II has the lower free energy and is thus the stable phase. Above $T_{I\text{-}II}$, Form I becomes the thermodynamically stable phase.

In general, polymorphic transformations do not occur at exactly the transition conditions but show hysteresis, that is, a difference in the transition temperature or pressure depending on whether the transformation is in the forward or the reverse direction [46,32,47]. Hysteresis results because of kinetic barriers to nucleation of the new phase [24,25]. At conditions close to the transition point, the energy barriers to nucleation may be considerable. The rate of transformation within the time period of the experiment is then too low as to be imperceptible to measurement. It is only when the conditions depart further away from the transition point that the transformation becomes sufficiently fast so as to be measurable. The extent of the transition barrier varies from substance to substance depending on the changes involved in the crystal structure on transformation. The extent of hysteresis in turn depends exponentially on the barrier and the rate at which the thermodynamic conditions (temperature, pressure etc.) are changed within a given experiment. For barriers less than $k_{\beta}T$ (where k_{β} is the Boltzmann constant and T the absolute temperature), any hysteresis may be experimentally indiscernible.

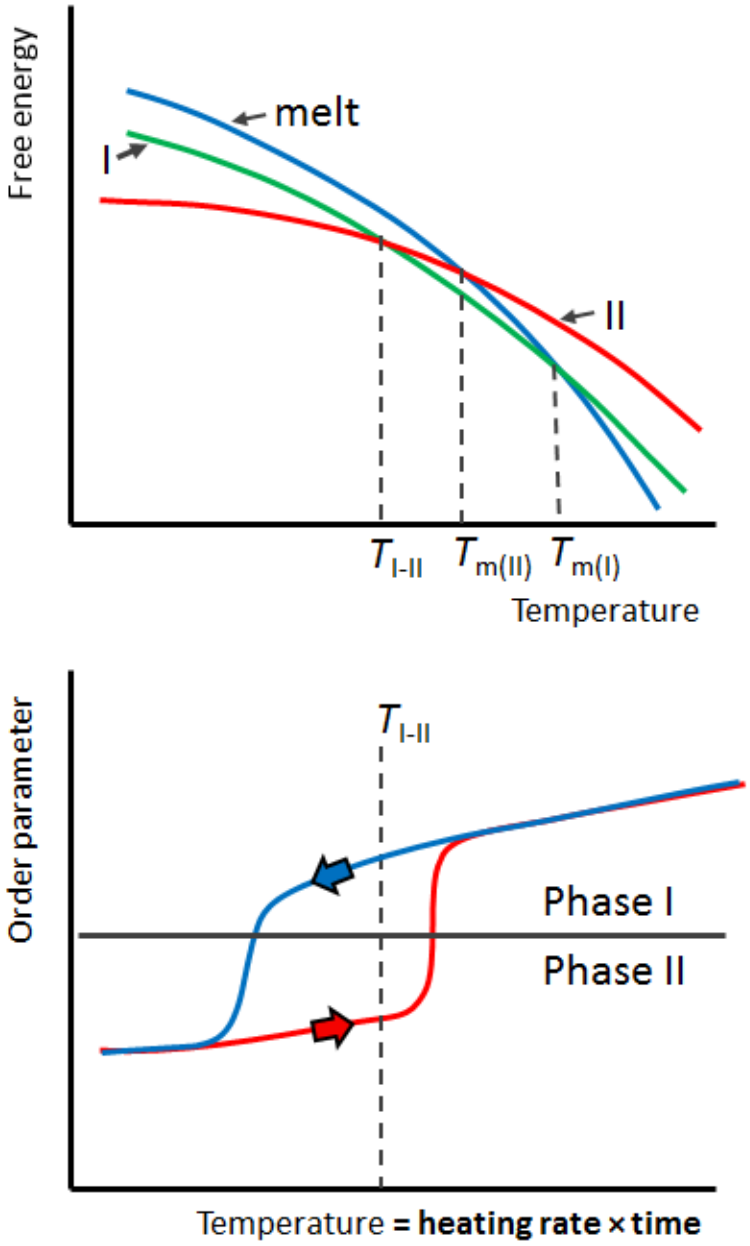

Figure 1. Top: free-energy surface of a hypothetical <u>enantiotropic</u> dimorphic system as a function of temperature. Bottom: Hysteresis of the *I*↔*II* transition when crossing the transition temperature $T_{I\text{-}II}$. The *II*-*I* and *I*-*II* transitions observed upon heating (red curve) and cooling (blue) respectively, are subject to nucleation barriers and thus experience kinetic trapping. Note that the centre of the hysteresis loop, commonly taken as the experimental transition temperature, needs not to coincide with the thermodynamic definition of the transition temperature i.e. at which $G_I = G_{II}$.

Polymorphic transitions are often also observed to be irreversible [12,25]. Throughout the conditions studied the transformation might be observed to proceed only in one direction. This may be because the reverse rate is too slow, or because the *G* surfaces of the phases concerned do not intersect and the one and same phase remains thermodynamically stable throughout right up to its melting point. If the latter is the cause, then the transformation is referred to as *monotropic*, in contrast to thermodynamically reversible transformations which are called *enantiotropic* [48,49]. Monotropic transformations are not subject to a transition temperature, but are controlled by kinetic factors. These transformations accordingly occur as a function of both temperature and time.

Forms that are thermodynamically unstable but can be isolated are termed *metastable*. Metastable forms once isolated can be quite stable; an extreme example being the diamond→graphite transition occurs at a rate of practically zero. The degree of metastability depends on the energy barriers to phase transition, which depend on the changes involved in bonding to form a nucleus of the stable form within the parent lattice.

3 Polymorphic phase transformations

3.1 Classification

Classification schemes which have been found to be particularly useful are those proposed by Ehrenfest [50], Buerger [51-53], and Ubbelohde [32,35]. Ehrenfest's classification is based on the behaviour of thermodynamic quantities, such as entropy, volume and heat capacity, at the transition point. The transitions are classed in terms of '*n*th order' where *n* is an integer given by the lowest derivative of Gibbs free energy *G* with respect to temperature *T* and pressure *p*, which shows a discontinuous change at the transition. Thus, a first order transition is defined as one in which a discontinuity occurs in the first derivative of the free energy. These derivatives correspond to entropy S (or latent heat of transition) and volume V respectively, viz.

$$G = \min\{G_I(T, p), G_{II}(T, p)\} \qquad -(2)$$

$$\Delta G = G_{II} - G_I = \Delta H - T\Delta S = \Delta U + p\Delta V - T\Delta S = 0 \quad \text{at transition point}$$

$$\left(\frac{\partial G_I}{\partial T}\right)_p = S_I \neq S_{II} = \left(\frac{\partial G_{II}}{\partial T}\right)_p \quad ; \quad \left(\frac{\partial \Delta G}{\partial T}\right)_p = -\Delta S = -\frac{\Delta H}{T} \neq 0 \qquad -(3)$$

$$\left(\frac{\partial G_I}{\partial p}\right)_T = V_I \neq V_{II} = \left(\frac{\partial G_{II}}{\partial p}\right)_T \qquad -(4)$$

Second order transitions do not involve entropy or volume changes, but are characterised by discontinuities in the second derivatives of free energy, that is heat capacity C_p, thermal expansivity κ, and compressibility β, whilst having continuous first derivatives.

$$\left(\frac{\partial^2 G_I}{\partial p^2}\right)_T = \left(\frac{\partial V_I}{\partial p}\right)_T = -V_I\beta_I \neq -V_{II}\beta_{II} = \left(\frac{\partial^2 G_{II}}{\partial p^2}\right)_T \qquad -(5)$$

$$\left(\frac{\partial^2 G_I}{\partial p \partial T}\right) = \left(\frac{\partial V_I}{\partial T}\right)_p = V_I\kappa_I \neq V_{II}\kappa_{II} = \left(\frac{\partial^2 G_{II}}{\partial p \partial T}\right) \qquad -(6)$$

$$\left(\frac{\partial^2 G_I}{\partial T^2}\right)_p = \left(\frac{\partial S_I}{\partial T}\right)_p = -\frac{C_p^I}{T} \neq -\frac{C_p^{II}}{T} = \left(\frac{\partial^2 G_{II}}{\partial T^2}\right)_p \qquad -(7)$$

Third and higher order transitions can be defined in principle by differentiating further.

The changes in the thermodynamic properties (as a function of temperature) at the transition point for first and second order phase transitions are shown in Figure 2. First order transitions show discontinuities in volume, enthalpy and entropy, and have infinite heat capacity at the transition. The heat capacity is infinite at the transition because it is given by the derivative of enthalpy with respect to temperature, that is, $C_p = \partial H / \partial T$, and the enthalpy shows a discontinuous change (Equation 3). Physically, the energy added to the system is utilised in driving the transition rather than on raising the temperature, and hence it represents the latent energy of the transition.

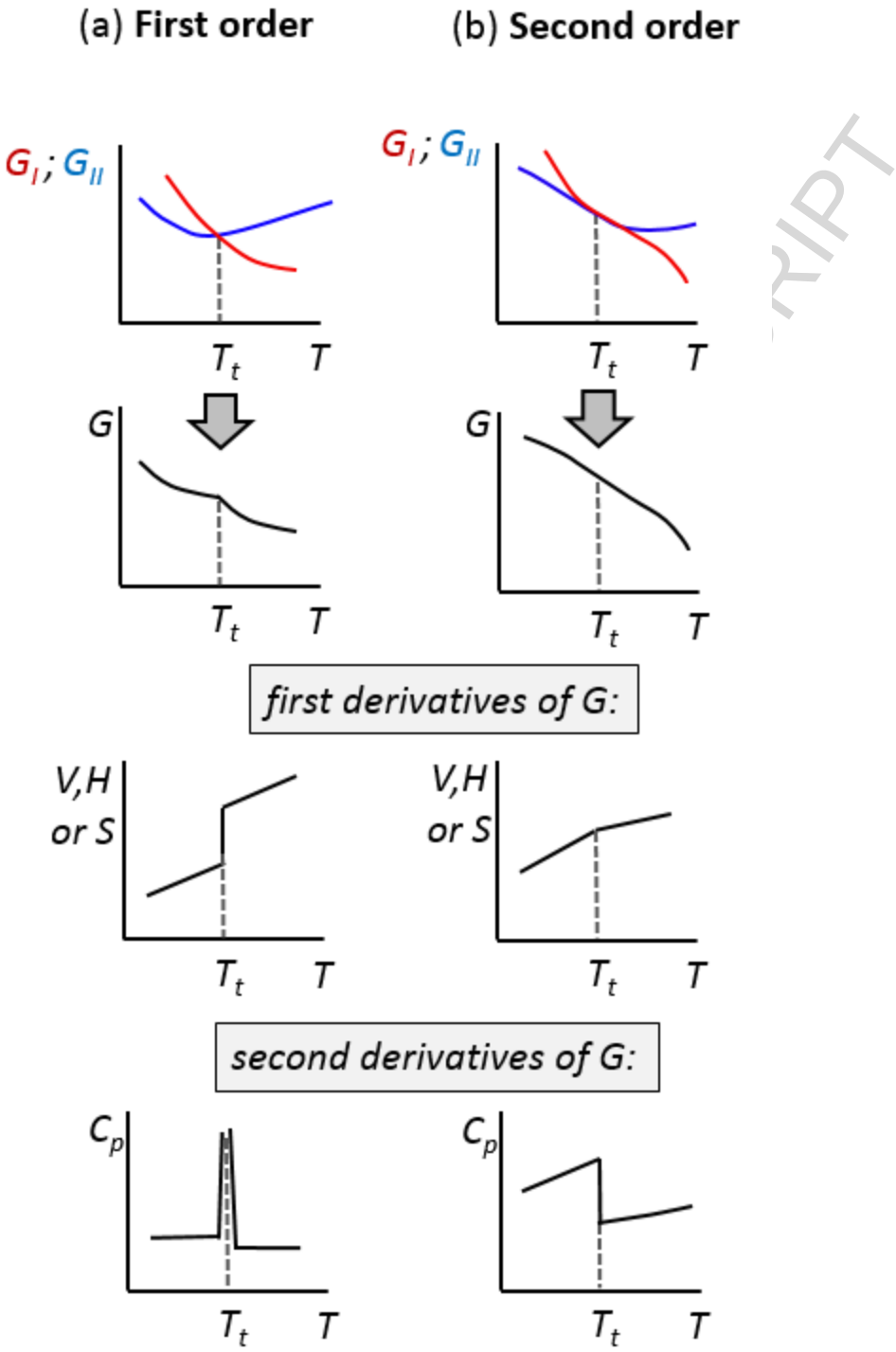

Figure 2. Variation of thermodynamic properties at the transition temperature T_t for first and second order phase transitions. The blue and red curves reflect the free energy of the low- and high-temperature phases *II* and *I*, respectively.

For second order transitions the gradient of Gibbs free energy is continuous, and the entropy and volume of the systems do not change. Since there is no entropy of transition ΔS, neither is there any enthalpy of transition ΔH. The important discontinuous thermodynamic function for second order transitions is that of heat capacity (see Figure 2).

It is difficult to visualise the nature of the free energy surface of second order transitions. Since the gradients (the first derivatives) of the free energy are continuous, the gradients of the free energy surfaces of the phases concerned are equal at the transition point. Hence, the surfaces cross at a sharp transition point as with first order transitions, but instead partially overlap at a transition regime (see Figure 2).

The scheme of Buerger is based on structural relationships between the crystal structures of the phases concerned. Transformations are classified on the basis of structural changes involving primary (nearest neighbours) or higher (next nearest neighbours) coordination, changes in type of bonding, and whether disorder is involved. An integral part of the scheme is the relationship between the structural changes involved and energy barriers affecting the kinetics of the transformations. The classification is given with examples in Table 1. Note the focus on inorganics.

Table 1. Classification of phase transformations according to Buerger [51]

Type of transition	Transition velocity	Example
First-coordination transformations		
(a) Reconstructive	sluggish	calcite-aragonite ($CaCO_3$)
(b) Dilatational	rapid	caesium chloride (CsCl)
Second-coordination transformations		
(a) Reconstructive	sluggish	quartz-cristobalite-tridymite (SiO_2)
(b) Displacive	rapid	high-low in SiO_2
Transformations involving disorder		
(a) Orientational	rapid	ferroelectric-paraelectric $NH_4H_2PO_4$
(b) Substitutional	sluggish	
Transformations of bond type	sluggish	grey-white tin

If the crystal structures are not similar, and the change from one structure to the other involves significant re-organisation of the atomic (molecules) species, requiring (inter-species) bonds to be broken and new ones to be formed, the transformation is considered to be reconstructive. Since bond breaking is involved, Buerger expects the energy barriers for such transformations to be high and the transformation rate to be sluggish.

Transformations involving subtler structural change in the first coordination are termed dilatation. Here no bonds are broken and the transformation is thought to occur by mere differential dilatation of the whole structure. Transformations of CsCl, NH_4Cl and NH_4Br, which are all relatively simple structures, are considered to occur by this mechanism. According to Buerger, as no bond breaking is involved, the energy barriers in dilatational transformations are

considered to be relatively small and the transformation rate (at a given driving force) to be rapid.

Transformations involving only the second coordination and where the crystal structures of the phases concerned are similar, such that going from one phase to another does not require breaking or making of bonds but rather distortion of bond angles and distances, are classified as displacive. Again, since only minor structural changes are involved, the energy barriers are considered by Buerger to be small.

Buerger's final category is that in which the crystal forms concerned differ greatly in the nature of bonding. Examples are polymorphs of tin (grey and white), where the character changes from semiconducting to metallic, and carbon (diamond-graphite), where the change is from an insulator to a semiconductor. Note that both of these transformations involve major structural changes and, therefore, could also be classified as reconstructive having large energy barriers.

Although Buerger's classification has become well established, it does appear to have some significant drawbacks. Firstly, the classification appears to have been developed with ionic and framework crystals in mind and mapping onto molecular crystals is not straightforward. For instance, molecular crystals rarely exhibit meaningful second coordination shells. Nevertheless, the terms displacive and reconstructive are now being used for phase transitions in molecular crystals, the former when the structural differences between the phases are minor, and the latter when the two phases differ in their hydrogen bonding networks. The use of the term `mechanism', to describe the observed geometrical relationships (for example, *distortion* and *dilatation* between the static crystal structures, is particularly unfortunate, being the cause of much confusion. Its use has implied that the geometrical relationships actually describe the structural changes taking place at the atomic/molecular level *during* a transition which we now know not to be the case.

Ubbelohde [32-35] divided phase transitions into continuous and discontinuous. In continuous transitions the crystal structure is expected to change smoothly and continuously from one form to another. In discontinuous transitions the structural change involved is not smooth. Although the classification is not based on any theoretical considerations, discontinuous transitions appear

to correspond to Ehrenfest's first order transitions and the continuous transitions to order-disorder type transitions.

Another class of transitions often discussed separately is that of martensitic transformations [24]. Although various observations are associated with this class, there appears to be no clear definition. Characteristics typically associated with martensitic transitions include velocity of transition being of the order of propagation of sound and independent of temperature (athermal), diffusionless and cooperative movement of atoms/molecules, definite orientational relationship between the lattices of the phases concerned, extent of transformation being dependent on the degree of cooling below the critical temperature, and transformation being affected by shear stresses. Another key stated feature is macroscopic change of shape of the transformed region. Some of these characteristics, however, are now being abandoned [24], and others do not offer any clear distinction. The reduced criteria appear to be that martensitic transitions (i) are first order, (ii) exhibit orientational relationships between the lattices, and (iii) and displacive shear of the lattice upon transformation gives rise to shape-change in the material. Martensitic transformations are observed in metals, alloys, and ceramics, and have significant technological applications that include manufacture of transformation-toughened materials, smart materials utilizing shape memory effects, and self-healing ceramics [29,54,55]. The term martensitic is derived from the transformation of the austenite form of iron (containing a small amount of carbon) by rapid quenching to yield the hard form of steel called martensite. A number of molecular crystals are known to exhibit martensitic-type characteristics e.g. hexamethylbenzene and DL-norleucine [56]. The transformation-induced shape change of martensitic materials implies the conversion of chemical energy to mechanical activity i.e. work. On this basis, thermosalient molecular crystals [15, and references therein; 57] (colloquially known as ‘jumping crystals’) in the act of jumping from a hot plate on transformation do mechanical work, and hence these transformations would be considered to be martensitic.

So, how do polymorphic phase transitions fit into these classification schemes? The transitions are invariably first order, and therefore local in nature occurring by nucleation and growth. They may or may not exhibit an orientational relationship between the lattices of the phases concerned. We do find the terms displacive and reconstructive useful, reflecting the nature of the lattice re-arrangements between the initial and final lattices and the potential link with kinetics.

We should add that until quite recently, structural concepts developed in the early last century combined with intuition of atomic bonding was the only way to estimate whether the energy barriers to nucleation were high or low. Using molecular simulations, as described below, we are now able to characterise phase transitions by computing both atomic pathways and *energy profiles*.

3.2 Molecular mechanisms

How do structural phase transitions occur at the molecular level? What actually happens to the molecules in time and space? This implies the elucidation of the 'reaction coordinate' – the mapping of the energetics and geometrical changes that occur in the course of a reaction, a seminal development by Eyring in 1935 [58]. However, whilst the implementation of this concept for solid-solid transformations is in principle straight-forward, in practice it is seriously complicated by the large number of molecules (atoms) involved. This particularly holds for molecular crystals which not only show displacements of molecular centres of masses, but also rotation and deformation of the molecular entities.

Mechanistic studies based on Buerger's ideas involve comparisons of the crystal structures of the polymorphs, and then a search for particular lattice transformations and molecular translations and rotations which link the structures. The molecular translations and rotations are then proposed as mechanisms for the transitions. A significant issue with this approach is that it suggests that the transitions occur homogenously via the proposed molecular translations and rotations throughout the bulk crystal. Such smooth transformation suggests that the free energy surfaces of the two phases overlap within an extended regime, i.e. refers to second order transitions (Figure 2)[59]. In contrast to this, first order transitions occur via nucleation and phase growth, and molecular organization occurring at the reactive interface for these transitions is unlikely to follow the structural changes proposed by Buerger-type analysis (see below in Section 5). This is also reflected by the final state found after a first order phase transition, as multiple nucleation events generally yield polycrystalline or domain structures with single crystal to single crystal transitions being exceptions and typically limited to small or nanocrystals [28,60].

There is now overwhelming evidence that all solid-state transformations of the first order kind occur heterogeneously by way of nucleation and growth [24]. Further, elegant experiments by Mnyukh and co-workers [56,61-66], on single crystals of molecular compounds, have shown that there is much similarity between the growth of a new phase in a solid-state transition and the growth of a crystal from a liquid or a gaseous phase. The studies involved direct microscopic observation, under maximum optical resolution, of single-crystal to single-crystal transitions, coupled with Laue x-ray diffraction on a variety of molecular crystals. For each compound, the crystals of the new phase (daughter), which grew within the parent crystals, exhibited facets with low crystallographic indices that were, in general, irrational relative to the parent lattice. The developing facets (representing the interface) also showed a series of steps such as those normally observed in crystals growing from the liquid or the gaseous phase. In general, no preferred orientation of the daughter crystals with respect to the parent lattice was observed, and a certain degree of superheating and supercooling was always found to be necessary to induce the transitions. This all strongly suggests that the *mechanics of polymorphic phase transitions are, in essence, similar to that of crystallisation* but with the difference that the bulk medium for the phase transitions is a crystalline lattice. For glutaric acid, the habit faces of the daughter crystals have indeed been observed to be the same as those of crystals grown from the melt [62].

The theory of nucleation in solids developed by Turnbull [67] is essentially an extension, to include effects of factors specific to condensed phases, of the theory proposed by Volmer and Weber [68] and Becker and Doring [69] for homogeneous crystal nucleation from the melt. At conditions just above the transition point, local fluctuations due to thermal agitation are thought to cause some atoms (or molecules) of the initial phase to take up structural positions corresponding to the product phase. The majority of these fluctuations result in the emerging periodic structure being below a certain critical size, and hence show a net increase in Gibbs free energy and are unstable. Only those fluctuations which lead to phase domains that exceed this critical size are capable of continued existence and become the nuclei of the product phase (the full thermodynamic account is given in Section 3.3). Growth of the new phase then reduces the net Gibbs free energy and proceeds by relocation of the molecules at the interface from the initial phase onto the nuclei. At the phase front, the molecular arrangements match neither the initial nor the final crystal structure and are thus energetically unfavorable. This local instability hence

propagates such that the transition process continues until the entire crystal has transformed to the new phase.

In real crystals, nucleation occurs at preferred sites such as edges, surfaces, grain boundaries, stacking faults, dislocations and point defects. Such deviations from the ideal lattice can considerably lower the necessary activation energy for the nucleation step. Indeed, these crystal imperfections appear to be a necessary condition reducing the hysteresis of polymorphic transitions. An extreme example illustrating this are high quality single crystals that only transform after defects are introduced by mechanical means, for example, by pin pricks [65].

At the phase front (the region where active rearrangement is taking place) it is thought (e.g. [63,25] that the process taking place is just simple relocation of the atoms/molecules from the initial to the product phase, and that there is no intermediate amorphous layer, as had been proposed by Hartshorne and co-workers [[70,71] and Bradley [72], but only a small gap (due to the mismatch between the lattices of the initial and the product phase) which is on average approximately half a molecular layer. The process is illustrated in Figure 3. The idea of the amorphous interface was discounted because the observed rates of transformations could never be reconciled with this postulate. In addition, results of experimental measurements and theoretical calculations (using the atom-atom potential method) of the tensile strength of the interface [65] have been found to be consistent with the above proposed mechanism, rather than with the existence of an amorphous layer. However, recent molecular simulations reveal that the molecular processes at the transformation interface do not always fall so neatly into this scheme. Depending on the nature of bonding, interfaces can be sharp, extended, even diffusive [59,73].

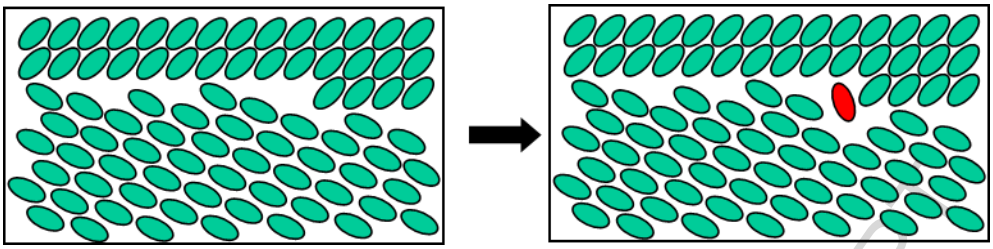

Figure 3. Proposed mechanism for the molecular rearrangement at the interface of a polymorphic transformation. Molecules detach one by from the parent phase and attach onto the surface of the emergent daughter phase. Energy considerations suggest that the process of detachment and attachment would occur on a molecule per molecule basis. This is akin to shifting a carpet by inducing a kink which is then propagated rather than wholesale shift of the carpet which is much more challenging. (Reproduced with permission from reference [127] J. Anwar, S. C. Tuble and J. Kendrick, J. Am. Chem. Soc., 2007, 129, 2542–2547; copyright 2007 American Chemical Society).

3.3 Kinetics

The rates at which polymorphic transitions occur vary enormously. Depending on the nucleation barrier, transitions may be extremely rare as, for example, the diamond to graphite transformation that occurs over geological timescales at ambient conditions. At the other extreme, many compounds show transformations that are so spontaneous that time-resolved experiments become challenging [74]. In developing the theoretical framework for kinetics, it is necessary to make a clear distinction between the two stages of transformation, i.e. nucleation and phase propagation, each of which is subject to a distinct energy barrier. Typically, the energy barrier for propagation is much smaller than that for nucleation. Indeed, the barrier to nucleation constitutes a conceptual maximum for the propagation energy barrier. As a consequence, phase front propagation can be very fast, even at the speed of sound - which is that of (elastic) density wave propagation in the crystal. An example of fast phase-front propagation in molecular crystals is that exhibited by DL-norleucine, where the rate of advance of the interface can be of the order of 10 cm/seconds even at very low superheating or supercooling [56].

The phase transition kinetics (for both nucleation and interface advance) have a certain dependence on the extent of superheating or supercooling (see Figure 4). The implication is that standard Arrhenius kinetics (that assume temperature-independent free energy barriers) are

poorly applicable. At temperatures very close to the transition temperature T_t, the net rate of transition is negligible (be it because of the structure being inert or because of balancing of the phase-front propagation in either direction). This temperature range over which the transformation rate is low corresponds to the hysteresis in the observed transition temperature. As the temperature is further removed from T_t the rate increases. For the transition driven by supercooling, the rate attains a maximum and then begins to decrease. For the superheating-induced transition, the rate continues to increase rapidly without any maximum. This behaviour is attributed to two causes: the dependence of the rate of nucleation and of interface advance on the extent of superheating or supercooling, that is, $\Delta T = (T–T_t)$, and on the absolute temperature T.

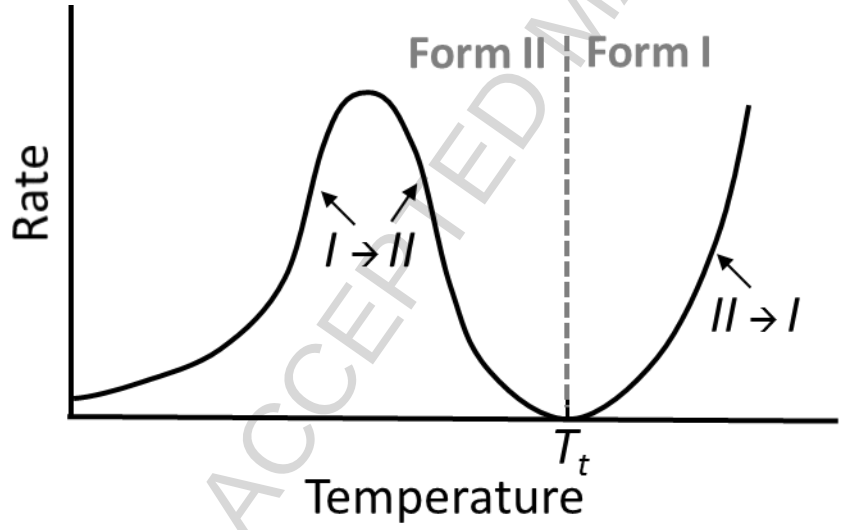

Figure 4. Temperature dependence of the transformation rate for the transformations *I→II* and *II→I* as observed below or above T_t, respectively. Note that the overall rate is mainly determined by that of nucleation, whilst interface advance for polymorphic phase transformations is typically relatively fast.

First order phase transitions are initiated by local nucleation events, resulting in budding of new phase domains, the nuclei, which then grow until the full crystal is transformed. The formation of nuclei results in the creation of new surfaces and, if volume change is involved (which it invariably is), stresses and strains. These make a positive contribution to the net free energy

change involved in the process of nucleation. The net free energy ΔG_N, therefore, does not simply equate to the free energy change due to the formation of the new phase within the nuclei ΔG_{bulk}, but is the combination of this and the free energy change due to the generation of the new interface $\Delta G_{\text{interface}}$, and associated strains ΔG_{strain} [67]. For nucleation to occur, ΔG_N must be negative.

$$\Delta G_N = \Delta G_{\text{bulk}} + \Delta G_{\text{interface}} + \Delta G_{\text{strain}} \qquad -(8)$$

The first term is negative while the second and third terms are positive. To a first approximation the strain term may be ignored (or, more precisely, implicitly considered as part of the bulk and interface terms). Indeed, it is intuitive to assume that a forming nucleus would adopt a shape such that shear stresses at its surfaces cancel out. The actual shape of a forming phase domain depends on the relation of parent and daughter lattices and may take the form of a cube, prism, or a complex polyhedra. For the sake of simplicity, the nucleation theory discussed in the following is elaborated for spherical nuclei. While nuclei in solid-solid transformation are typically not spherical, this is still the most commonly used model. The general physics discussed below may be transferred to all shapes as analogous expressions can be developed for any regular shape. Then for a spherical nucleus of radius r the explicit form of ΔG_N is

$$\Delta G_N = \frac{4}{3}\pi r^3 \Delta g_V - 4\pi r^2 \gamma \qquad -(9a)$$

The corresponding expression for a cubic nucleus of dimension a would read:

$$\Delta G_N = a^3 \Delta g_V' - 6a^2 \gamma' \qquad -(9b)$$

where Δg_V is the bulk free energy per unit volume and γ is the surface free energy per unit area.

$$\Delta g_V = \frac{\Delta G_{bulk}}{V_{nucleus}} = \begin{cases} \dfrac{G_{II} - G_I}{V_{nucleus}^{II}} & I \to II \quad (T < T_t) \\ \dfrac{G_I - G_{II}}{V_{nucleus}^{I}} & II \to I \quad (T > T_t) \end{cases} \qquad -(10)$$

From the expression 9a, it is clear that for small radii r the second term (that due to the interface) will dominate, and since its contribution is positive, ΔG_N will be positive. Consequently, any embryo that might form with a radius below some critical size will be thermodynamically unstable and hence will disperse. With increasing r, ΔG_N goes through a maximum at $r = r_c$, the critical radius, and then begins to decrease as the bulk free energy term begins to dominate. The variation of ΔG_N as a function of the radius at a number of different temperatures is shown in Figure 5. At $r = r_d$, ΔG_N goes through zero and for $r > r_d$ it is negative. Nuclei with $r > r_d$ become stable crystals. Embryos with r between r_c and r_d are metastable nuclei – they are thermodynamically unstable since ΔG_N is positive but would require a re-crossing of the nucleation barrier to dissolve. Consequently, the down-hill move to larger and thus more stable nuclei is preferred.

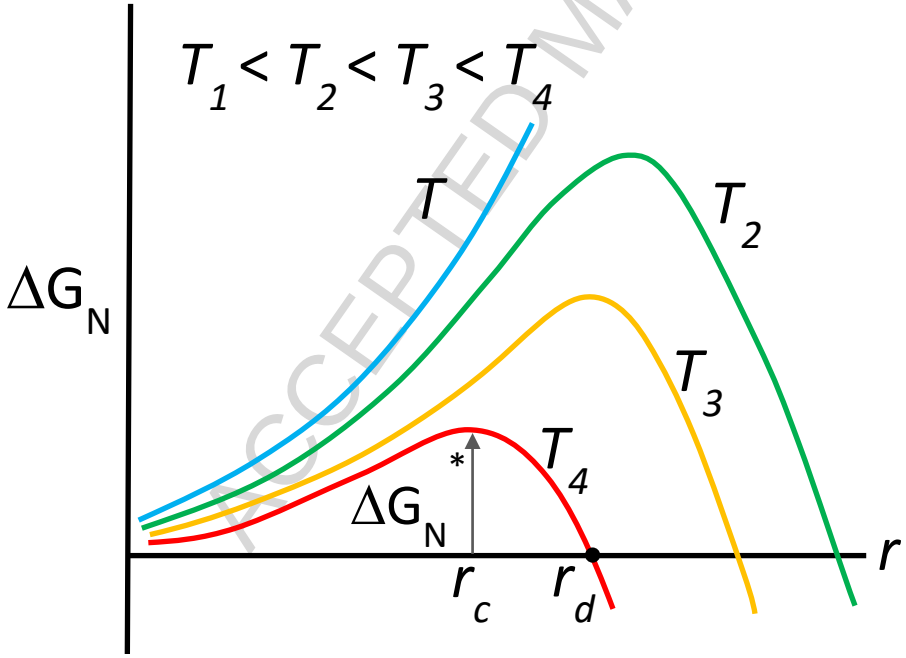

Figure 5. Variation of the free energy change for nucleation ΔG_N as a function of radius r at various temperatures. ΔG_N^* is the critical free energy characterizing a nucleus with a critical radius r_c.

Expressions for the critical radius r_c and the critical excess free energy ΔG_N^* can be obtained by using the necessary condition of $\partial \Delta G_N / \partial r = 0$ and rearranging for r_c:

$$r_c = \frac{2\gamma}{\Delta g_V} \qquad -(11)$$

and substituting this into Equation 9a

$$\Delta G_N^* = \frac{16\pi\gamma^3}{3\Delta g_V^2} \qquad -(12)$$

To a first approximation the dependence of γ on temperature may be ignored. Δg_V, as it may be seen below, whilst zero at T_t, is however proportional to $(T\text{-}T_t)$ at other temperatures. At temperature T_t

$$\Delta G = G_{II} - G_I = \Delta H - T_t \Delta S = 0 \qquad \text{or, if written per volume unit,}$$

$$\Delta g_V = \frac{\Delta G}{V_{nucleus}} = \Delta h - T_t \Delta s = 0$$

So,

$$\Delta S = \frac{\Delta H}{T_t} \quad \text{and} \quad \Delta s = \frac{\Delta h}{T_t} \qquad -(13)$$

Therefore, at any other temperature T (substituting into the Gibbs free energy function i.e. Equation 1 and assuming ΔH and ΔS do not change with temperature – hence the reason for the non-exact term)

$$\Delta G \cong \Delta H - T\frac{\Delta H}{T_t} = \frac{\Delta H}{T_t}(T_t - T)$$
$$\Delta g_V \cong \frac{\Delta h}{T_t}(T_t - T) \qquad -(14)$$

Substituting this into Equations 11 and 12 gives

$$r_c = -\frac{2\gamma T_t}{(T_t - T)\Delta h} \qquad -(15)$$

$$\Delta G_N^{\,*} = \frac{16\pi\gamma^3 T_t^{\,2}}{3\Delta h^2 (T_t - T)^2} \qquad -(16)$$

where Δh is the enthalpy change per unit volume of the phase transition.

Hence, the critical radius r_c is inversely proportional to $\Delta T = T - T_t$. At temperatures close to T_t, $\Delta g_V \to 0$ and r_c becomes infinitely large. Consequently, nucleation cannot occur at T_t. On increasing ΔT the magnitude of r_c and the free energy barrier $\Delta G_N^{\,*}$ decrease, resulting in an increase, within a given time, in the population of embryos which go on to become stable nuclei. The rate of nucleation, therefore, increases with increase in the degree of superheating or supercooling.

Consider now the effect of absolute temperature on the nucleation rate. The rate of nucleation is given by the product of the population of the critical-sized embryos that may be present and the probability (frequency) of their conversion to the new phase. If the number of embryos present in the parent phase are N_0, then from Boltzmann statistics the number of these which are of critical size (N_c) can be approximated by

$$N_c = N_0 \exp\left(\frac{-\Delta G_N^{\,*}}{k_B T}\right) \qquad -(17)$$

where k_B is the Boltzmann constant.

The conversion of critical-sized embryos to stable nuclei requires the transfer of at least one atom or molecule across the interface onto the embryo. Such transfers or jumps are subject to the activation energy G^* of phase-front propagation. For the transformation of phase *II* to *I*, if the embryos of emerging phase *I* are surrounded by *n* atoms (or molecules) at the interface, the

frequency $\nu_{\text{growth step}}$ with which the atoms (or molecules) cross the interface and attach to the embryo is given by

$$\nu_{\text{growth step}} = \nu \exp\left(-\frac{G^*_{II\to I}}{k_B T}\right) \qquad -(18)$$

where ν is the lattice vibration frequency, and $G^*_{II\to I}$ is the free energy of activation for the transfer of atoms (or molecules) of phase *II* to the emerging nuclei of phase *I* (see Figure 6).

The rate of post-critical nuclei formation (per unit volume per unit time) is the product of the population of critical-sized embryos and their rate of conversion to stable nuclei and is therefore given by

$$\frac{dN_{C+}}{dt} = N_0 \nu \exp\left(-\frac{\Delta G_N{}^* + G^*_{II\to I}}{k_B T}\right) \qquad -(19)$$

where $G^*_{II\to I}$ reflects the kinetic barrier to phase propagation in the $II \to I$ direction, whilst $\Delta G_N{}^*$ describes the thermodynamic disfavoring of forming a nucleus of critical size of the new phase.

The nucleation rate predicted by this expression as a function of temperature takes the form shown in Figure 4. At T_t the rate is zero. In the temperature region below T_t it passes through a maximum and then tends to zero at 0K. Above T_t the rate increases rapidly with temperature. The cause of this characteristic variation is the temperature dependency of $\Delta G_N{}^*$ described earlier (Equation 16).

Once a post-critical nucleus is formed, the transformation kinetics then depend on the rate of *phase propagation* (interface advance). The effect of temperature on the rate of phase propagation can also obtained from transition state theory. Here we follow and build on the formalism developed by Young [75] and Rao and Rao [25]. In full analogy to the above discussion, the advance of the interface is considered to be via an atom-by-atom (or molecule-by-molecule) transfer across the interface between the two phases, with the transfers or jumps being restricted by a free energy barrier. The latter is $G^*_{II\to I}$ for the forward $II \to I$ direction (phase

propagation in favor of the more stable phase) and $G^*_{I\to II}$ for the reverse $I\to II$ process (see Figure 6). Note that $G^*_{II\to I} + (-\Delta G_{I\text{-}II}) = G^*_{I\to II}$ and when $\Delta G_{I\text{-}II} < 0$ i.e. $T > T_t$, the barrier for back-propagation ($I\to II$) is larger than for the forward direction i.e. $G^*_{II\to I} < G^*_{I\to II}$.

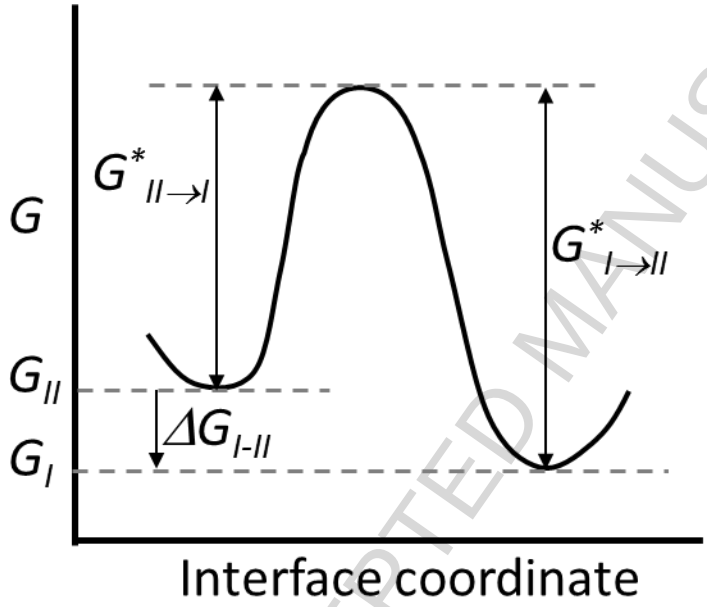

Figure 6. Free energy barriers to transfer of molecules across an interface. Note that $G^*_{II\to I} + (-\Delta G_{I\text{-}II}) = G^*_{I\to II}$.

Consider the transition of phase *II* into phase *I* (net growth of phase *I*). The number of atoms (or molecules) transferred from phase *II* to *I* via the interface area *A* per unit time may be written as

$$\frac{dN_{II\to I}}{dt} = A\cdot n_{II}\, p_{II\to I}\nu_{II}\exp\left(-\frac{G^*_{II\to I}}{k_B T}\right) \qquad -(20)$$

where n_{II} is the number of atoms (or molecules) per unit area of phase *II* at the interface, ν_{II} is the frequency of atom (molecule) vibration normal to the interface and $p_{II\to I}$ is the probability that this vibration is directed towards a lattice site of phase *I*.

Similarly, the number of atoms (or molecules) leaving phase *I* is given by

$$\frac{dN_{I\to II}}{dt} = A\cdot n_I\, p_{I\to II}\nu_I \exp\left(-\frac{G^*_{I\to II}}{k_B T}\right) = A\cdot n_I\, p_{I\to II}\nu_I \exp\left(-\frac{\left(G^*_{II\to I}-\Delta G_{I-II}\right)}{k_B T}\right) \qquad -(21)$$

The net transfer of atoms (molecules) into phase I is

$$\frac{dN_I}{dt} = A\cdot n_{II}\, p_{II\to I}\nu_{II} \exp\left(-\frac{G_{II\to I}{}^*}{k_B T}\right) - A\cdot n_I\, p_{I\to II}\nu_I \exp\left(-\frac{G_{II\to I}{}^* - \Delta G_{I-II}}{k_B T}\right) \qquad -(22)$$

At phase coexistence, phase fronts may be subject to fluctuations, but no net growth of either phase occurs. As $\Delta G_{I\text{-}II} = 0$ the two exponential terms become identical and the coexistence condition reads:

$$0 = \frac{dN_I}{dt} \quad at\ \ T = T_t \quad \rightarrow \quad n_{II}\, p_{II\to I}\nu_{II} = n_I\, p_{I\to II}\nu_I \qquad -(23)$$

In other terms, the differences in density *n* and vibrational frequency υ in phases *I* and *II* is compensated by the different probabilities $p_{II\to I}$ *and* $p_{I\to II}$ that a spontaneous vibration locks into a lattice site of phase *I* and *II*, respectively.

To rationalize this issue, consider for example the case of $n_I < n_{II}$. For a successful jump from phase *I* to phase *II*, atoms (molecules) will need to leave a comparably large volume and lock into a smaller one. For an individual jump across the interface, chances to reach a suitable lattice site are thus $p_{I\to II} < p_{II\to I}$. However, the denser phase II offers more candidates for such jumps, effectively balancing the net transformation rate at ΔG=0. It is intuitive to assume $n_{II}\, p_{II\to I}\nu_{II} \approx n_I\, p_{I\to II}\nu_I$ to hold as a good approximation beyond the phase coexistence line, i.e. for $\Delta G \neq 0$, and what follows will be based on this consideration.

The net speed of phase interface propagation may be deduced from the increase of a nucleus volume as a function of time

$$\frac{dx}{dt} = \frac{d}{dt}\left(\frac{V_{nucleus}}{A}\right) = \frac{1}{\rho_I}\cdot\frac{d}{dt}\left(\frac{N_I}{A}\right) \qquad -(24)$$

where ρ_I is the number density of phase *I*. Using the above considerations, we get

$$\begin{aligned}\frac{dx}{dt} &= \frac{1}{\rho_I}\left[n_{II}\,p_{II\to I}\nu_{II}\exp\left(-\frac{G_{II\to I}^{*}}{k_BT}\right) - n_I\,p_{I\to II}\nu_I\exp\left(-\frac{G_{II\to I}^{*}-\Delta G_{I-II}}{k_BT}\right)\right] \\ &= \frac{1}{\rho_I}n_{II}\,p_{II\to I}\nu_{II}\exp\left(-\frac{G_{II\to I}^{*}}{k_BT}\right)\cdot\left[1-\exp\left(\frac{\Delta G_{I-II}}{k_BT}\right)\right]\end{aligned} \qquad -(25)$$

which is commonly written as

$$\frac{dx}{dt} = k(T)\left[1-\exp\left(-\frac{\Delta G_{I-II}}{k_BT}\right)\right] \qquad -(26)$$

where $k(T)$ is the temperature-dependent rate constant for the atomic jump across the interface triggered by the activation energy $G_{II\to I}$* for forward propagation of the phase front.

$$k(T) \approx \text{const}\cdot\exp\left(-\frac{G_{II\to I}^{*}}{k_BT}\right) \qquad -(27)$$

This rate constant relationship is similar to the classical Arrhenius equation.

Equation (25) predicts that at T_t, since $\Delta G_{I\text{-}II} = 0$ and $\exp(\Delta G_{I\text{-}II}/k_BT) = 1$, the net speed of phase front propagation is zero. At moderate favoring of the phase transition, ΔG is negative but small and $\exp(\Delta G_{I\text{-}II}/k_BT) < 1$, hence the rate will also be low. With increasing thermodynamic driving of the *II*→*I* transition, $\Delta G_{I\text{-}II}$ gets increasingly negative and $G^{*}_{II\to I} << G^{*}_{I\to II}$, thus leading to a diminishing rate of back-propagation. For $\Delta G_{I\text{-}II} \to -\infty$, $\exp(\Delta G_{I\text{-}II}/k_BT) = 0$, and equation (25) formally predicts a speed limit – which may be associated with the speed of sound within the parent phase *II*, i.e. the maximum speed of any mechanical action applied to the solid.

If the transition is induced by *supercooling*, fast phase-front propagation driven by maximum ΔG potential is counteracted by a decrease in the temperature-dependent rate constant $k(T)$ due to the

drop in temperature. The equation, therefore, predicts that with an increase in supercooling, there is a maximum in the phase transformation rate followed by a decrease. The location of this maximum depends on both, the thermodynamic favoring of the transition ΔG and the barrier to phase front propagation G^*, which in principle can be deduced from experiment using Equations 26 and 27. On the other hand, on *superheating* the rate of the transformation increases rapidly with no maximum predicted, with both the thermodynamic potential ΔG and the temperature-dependent rate constant $k(T)$ acting in concert. An illustrative example of this kinetic behavior of interface advance is exhibited in single crystals of p-dichlorobenzene as a function of ΔT [61].

In typical kinetic studies of phase transitions, see e.g. [76], it is normally assumed that the effect of temperature on the rate of interface advance is solely due to its effect on the rate constant as given by the Arrhenius equation. From the foregoing discussion, it is clear that this is only true at temperatures well away from T_t. This conclusion is indeed borne out in experimental studies, see e.g. [77,78].

The characterisation of bulk kinetics of phase transitions in the solid state is fundamentally different from that in the liquid or the gaseous phase. In the solid state the important conventional concepts of concentration, order of reaction or molecularity have little or no application. Instead, because of the relative immobility of the constituent atoms or molecules, the kinetics are governed by topochemical factors (n, p and v in Equation 20).

Ideally, in common with interface-controlled solid state reactions, the fundamental parameters in solid phase transitions are the rate of nucleation characterized by the rate constant k_N, the spatial distribution of the formed nuclei, that is, whether the nuclei are confined to the surface or occur throughout the bulk crystal, and the rate of subsequent advance of the formed interface, characterized by the rate constant k_G. The rate of interface advance may be anisotropic, being characteristic for the different crystallographic directions in the crystal $k_G^{(hkl)}$. Coupled to the temperature-dependent rate constants are the temperature-independent activation energies E_N^*, $E_G^{*(hkl)}$). Nucleation may be instantaneous, or its rate may follow a linear, exponential, or another power law. The progress of interface advance is, to a first approximation, usually linear with time, governed by a maximum speed given by that of sound along the corresponding cystallographic direction [79]. Further, finite size effects may be crucial for materials that either exhibit domain structure or occur as discrete crystallites.

In practice, the kinetics are often further complicated and not always quantitatively reproducible [66]. Irreproducibility, in the main, stems from the variation in crystal perfection. Both nucleation and the rate of interface advance are markedly dependent on defects in the crystal. In a good quality crystal, that is, one with few defects, nucleation is difficult if not impossible. If, however, certain defects are introduced artificially, for example, by means of pin pricks, then nucleation at these defects is almost instantaneous even at very low superheating or supercooling. Likewise, the rate of interface advance can also show considerable variation depending on the quality of the crystal, and may not always be linear with time: it may increase or decrease with time or on recycling, or show stop-start or rapid burst behavior. Such behaviour is again attributed to defects. Acceleration of the rate of interface advance is thought to occur as a result of defects accumulating ahead of the interface, whilst rapid-bursts, deceleration or temporary stoppage are considered to be caused by the release of strain built up at the interface; the rapid bursts occurring due to generation of defects ahead of the interface possibly initiating additional nucleation sites, and stoppages because of disturbance of the proper contact between the two forms at the interface – an example of the latter being stacking fault formation [74].

Work on single crystals of p-dichlorobenzene [61] has shown that the velocity of interface advance can also be dependent on the number of cycles of transition that a crystal has undergone. With an increasing number of transitions the velocity was observed to decrease. This was explained as being due to depletion of defects with each cycle, the defects being consumed by the interface and then released at the crystal surface. The velocity was also influenced by the presence of other interfaces nearby; it increased greatly as the approach distance between the interfaces became less than about 1.5mm. Buildup of defects at the interface and their transport into the region between was proposed as the explanation.

Experimental determination of the kinetic parameters is best carried out on single crystals using direct microscopic observation. This, however, may be either impossible because of a lack of single crystals, or inappropriate when, for example, kinetic parameters are required for a polycrystalline or a powdered sample. When single crystals are not available, the fundamental kinetic parameters cannot be determined directly. Experimentally, only the overall rate in terms of the fraction of material transformed $\alpha(t,T)$ as a function of time and/or temperature is accessible. This α–time curve is typically sigmoid in appearance. The problem, therefore, is that

of extraction of the fundamental parameters for a given sample from the overall rate data (α–time curve). The task is complicated further because the overall rate is strongly dependent on the crystal morphology, crystal size and size distribution as well as crystal perfection. Moreover, changes in shape, the degree of poly-crystallinity and even fragmentation may result from polymorphic transitions themselves, thus complicating experimental reproducibility even further.

The modelling of solid state kinetic data to a large degree is a problem in solid geometry. In developing an expression that describes the overall rate of a polymorphic transition one needs to take into account: (i) crystal morphology, size and size distribution; (ii) spatial distribution of the nuclei; (iii) appropriate nucleation rate law and corresponding rate constant; (iv) rate of interface advance, which usually can be assumed to be linear with time but may be anisotropic, being characteristic for the individual crystal facets of the new phase; and (v) correction for the ingestion of potential nucleation sites and the contact/coalescence of the growing nuclei, which results in reduction/loss of reactive interface as the reaction proceeds to completion.

The development of a generalised kinetic expression, therefore, is not a trivial task. Consequently, a number of equations for specific cases have been developed [80-84]. Of these, probably the most successful is that proposed by Avrami [80-82]. This takes the form

$$\alpha = 1 - \exp\left(-kt^n\right) \qquad -(27)$$

where k is the overall transformation rate constant, and $1 \leq n \leq 4$ depending on the spatial distribution and the rate of nucleation.

When dealing with powdered samples comprising very small particle size, the Avrami model may not apply. The Avrami model assumes that potential nuclei of the new phase are randomly distributed throughout the bulk of the crystal, and that these nuclei, once activated, grow throughout the old phase until the transformation is complete. When a crystal is progressively subdivided (i.e. comminuted or powdered), there comes a stage when there will be only a few potential nuclei within each *crystallite*. As the rate of nucleation is considered to be proportional to the number of potential nuclei present, the transformation will, therefore, become nucleation controlled. Consequently, the overall kinetics may not comply with the Avrami model, since the

transformation due to any nucleation event will be constrained to the particular crystallite within the powder.

Further, for powdered samples, the phase transformation often does not go to completion, with the maximum fraction (α_{max}) transformed depending on the extent of superheating or supercooling [85,86]. The cause here is that some of the crystallites do not have potential nuclei that can be activated at the particular temperature of study, and hence the transformation does not proceed to completion. Higher temperatures are able to activate the higher activation energy nuclei, bringing additional crystallites into the transformation. Consequently, α_{max} depends on the temperature, with higher temperatures leading to higher values of α_{max} [86,87]. Clearly, for powder samples there is a need to incorporate a distribution of activation energies in the kinetic model [86,88].

In summary, characterisation of the kinetics of polymorphic phase transformations, particularly transformations in powders, is complex. For powders, usually only a single overall activation energy can be estimated, and this by itself, because it contains contributions from nucleation events and phase growth, conveys no rigorous mechanistic insight. In addition, because of thermodynamic considerations the data will invariably depart from ideal Arrhenius behaviour, especially at temperatures close to phase coexistence. Finally, the data may be irreproducible from sample to sample, because of variation in crystallite size, shape, quality or history.

4 Molecular simulation of polymorphic phase transitions

4.1 Molecular simulation methodology

Possibly the simplest simulation approach to studying phase transition phenomena is the Ising model and its generalization, the Potts model [23]. The Ising model consists of discrete elements on a lattice that represent magnetic dipole moments of spins, with each element for instance representing a crystallite/domain (Figure 7). The spin in each element can be either up or down and would be influenced by the spin in its neighbouring (interacting) elements and any external field. Phase transitions can be induced and their development tracked by monitoring the spins as

they undergo realignment, to yield the new phase consistent with the applied field. These models have contributed extensively to our generic understanding of phase transitions.

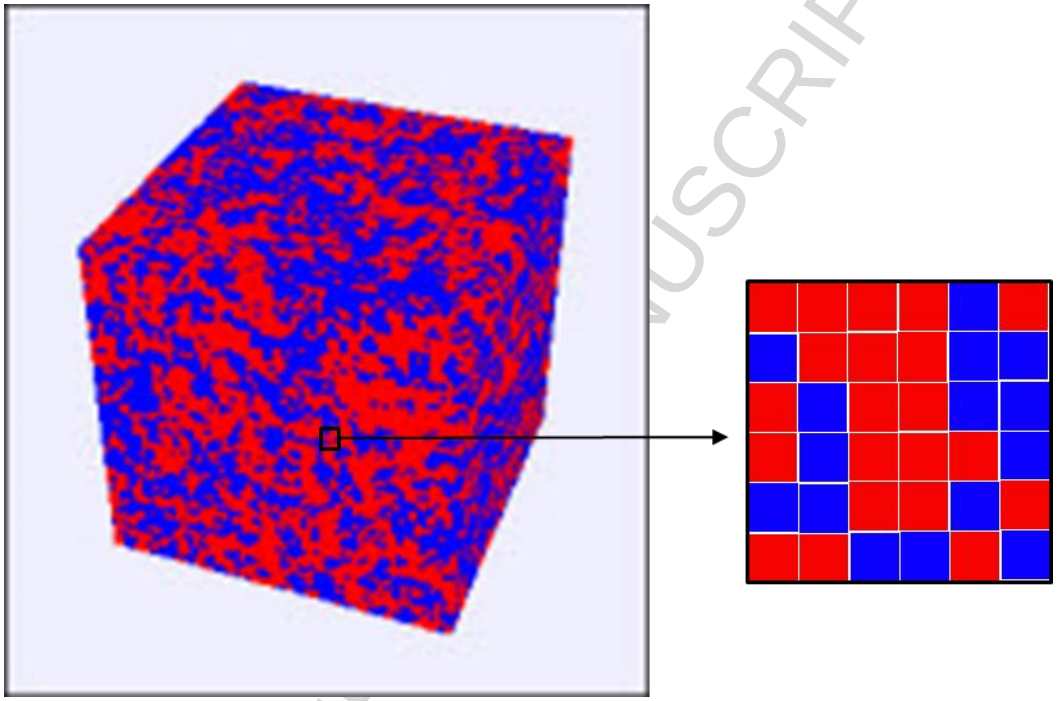

Figure 7. Ising model simulation of magnetization. The volume elements or domains can be either spin up (red) or spin down (blue). The outcome of a particular domain is influenced by the spins of the nearest neighbor domains and any external potentials such an external magnetic field or temperature. The simulation image is from Wolfgang Christian's (Davidson College) 3D checkerboard Decomposition Model code [89], and is reproduced here with permission.

Molecular simulation may be perceived to be a significant step up in complexity from the Ising/Potts models. The interacting volume elements of these simple models are replaced by molecules which are free to translate, rotate and flex, making molecular simulation an 'off-lattice' technique. Further, the element-element interactions give way to intermolecular forces between the atoms, which determine their dynamics and simulations track the trajectories of the molecules as a function of time. Molecular dynamics simulation therefore serves as an atomic microscope revealing the temporal changes in molecular organisation. Molecular simulations can be carried out at constant temperature and pressure (*NpT* ensemble), hence mimicking conditions

in the laboratory. The implication is that the simulations (in principle) converge to lowest free energy state, akin to real systems. The temperature and pressure, being the primary potentials of interest driving phase transitions, can be set as required.

Molecular simulations offer a number of methods and approaches to predicting and rationalizing phase stability and polymorphic transitions. For a given molecular arrangement (configuration), the best accuracy in terms of structure, energies and interaction forces is achieved by quantum chemistry. The downside of using such a high level of theory is the immense computational demand, which means that quantum chemistry calculations are restricted to small model systems and only limited sampling of the manifold of different configurations. To assess larger systems and extended statistics, it is necessary to employ the computationally inexpensive, lower-resolution approximation termed molecular mechanics. This comprises empirical interaction potentials, commonly referred to as a force field [90,91], to describe the interaction forces. The most common source for defining force field parameters is quantum mechanical calculations performed for a single molecule in the gas phase to characterize molecular flexibility and for dimers (or oligomers) of molecules to characterise non-bonded intermolecular forces, respectively. Replacing quantum mechanics by molecular mechanics i.e. methodology based on force fields, enable simulations comprising millions of molecules to be carried out for up to microseconds of simulation time.

The definition and parameterisation of a force-field reflects a coarsening of quantum mechanical models, such as approximating diffuse electron density distribution within molecules by point charges placed on the atoms. While this reflects a reasonable simplification of molecular electrostatics, further potential energy terms are added to mimic electronic polarization. In many cases, the interplay of electrostatics, van-der-Waals interactions and atomic repulsion stemming from overlapping electron density, is mimicked by three simple functions, using q_i, q_j, A_{ij} and B_{ij} as adjustable parameters.

$$\left\langle \hat{H} \right\rangle_{quantum\ mechanics} \cong \sum_{i,j} V\left(r_{ij}\right)_{molecular\ mechanics} = \sum_{i,j} \frac{q_i \cdot q_j}{4\pi r_{ij}} + \frac{A_{ij}}{r_{ij}^{12}} - \frac{B_{ij}}{r_{ij}^{6}} \qquad -(28)$$

where r_{ij} represents the separation distance between atoms i and j, and q_i are q_j partial charges on atoms i and j. Similarly, molecular flexibility is mimicked by assigning harmonic springs to characterise bonds and valence angles, and by employing periodic potential energy terms (often

based on cosine functions) to describe the energy profile of torsional degrees of freedom (rotations about bonds). The typical full potential energy function is given in Figure 8.

$$U = \sum_{i<j} \sum 4\varepsilon_{ij}\left[\left(\frac{\sigma_{ij}}{r_{ij}}\right)^{12} - \left(\frac{\sigma_{ij}}{r_{ij}}\right)^{6}\right]$$

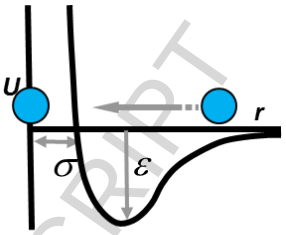

$$+ \sum_{i<j} \sum \frac{q_i q_j}{4\pi\varepsilon_0 r_{ij}}$$

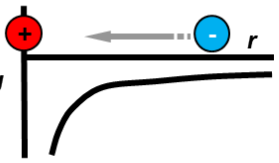

$$+ \sum_{bonds} \frac{1}{2} k_b (r - r_0)^2$$

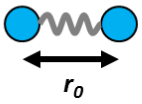

$$+ \sum_{angles} \frac{1}{2} k_a (\theta - \theta_0)^2$$

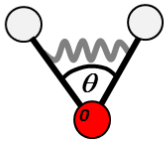

$$+ \sum_{torsions} k_\phi \left[1 + \cos\left(n\phi - \delta\right)\right]$$

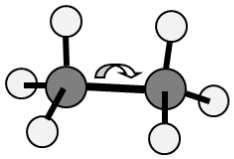

Figure 8. The molecular mechanics potential energy function comprising the van der Waals (term 1, Lennard-Jones) and coulombic (term 2) interactions, and the three valence terms, bond, angle bending, and dihedral energy. The summations for van der Waals and coulombic terms indicate all pairwise interactions between atoms that are not either bonding or linked via a bond angle. The Lennard Jones parameters ε_{ij} and σ_{ij}, partial charges q_i and q_j, and the force constants k_b, k_a, and k_ϕ are all atom-specific parameters that comprise the force field and are inputs to the simulation.

In molecular dynamics simulations the time evolution of a given molecular system is simulated by solving Newton's equations of motion for the atomic interaction forces as derived from the potential energy representation (Figure 8). As the continual interaction of molecules prohibits an analytical solution, the molecular dynamics simulation technique uses an approximation valid only for short time intervals Δt.

$$-\frac{d}{d\vec{r}_i}\left(\langle H\rangle_{qm} \text{ or } V_{mm}\right)=\vec{F}_i=m_i\cdot\frac{d^2}{dt^2}\vec{r}_i\cong m_i\frac{\vec{r}_i(t+\Delta t)-2\vec{r}_i(t)+\vec{r}_i(t-\Delta t)}{\Delta t^2} \qquad -(29)$$

$$\rightarrow\quad \vec{r}_i(t+\Delta t)\cong 2\vec{r}_i(t)-\vec{r}_i(t-\Delta t)+\frac{\vec{F}_i}{m_i}\Delta t^2 \qquad (\Delta t=0.1-2\,fs)$$

where t and m_i represent time and atomic mass, respectively. The time evolution of the atomic positions is calculated from the second line of Equation 29. Depending on the model system and the applied temperature, the underlying approximation is limited to time step Δt of about 2 femtoseconds (10^{-15} s) or lower. Thus for assessing longer trajectories, Equation 29 is employed iteratively with updates of the positions and forces being calculated after each time step to evolve the system forward in time (Figure 9). Given that each force calculation uses a certain amount of cpu and evolves the system by only ~ 10^{-15} s, a typical simulation on a high-performance computing facility can take days to carry out the billions or trillions of force calculations to evolve the molecular system to nano- or micro-second time scale. This limited time scale (of the order of microseconds) is a major limitation of standard (brute force) molecular dynamics simulation. However, there are now enhanced sampling techniques that are able to simulate phase formation and transitions that are beyond such time scales (see Section 4.3).

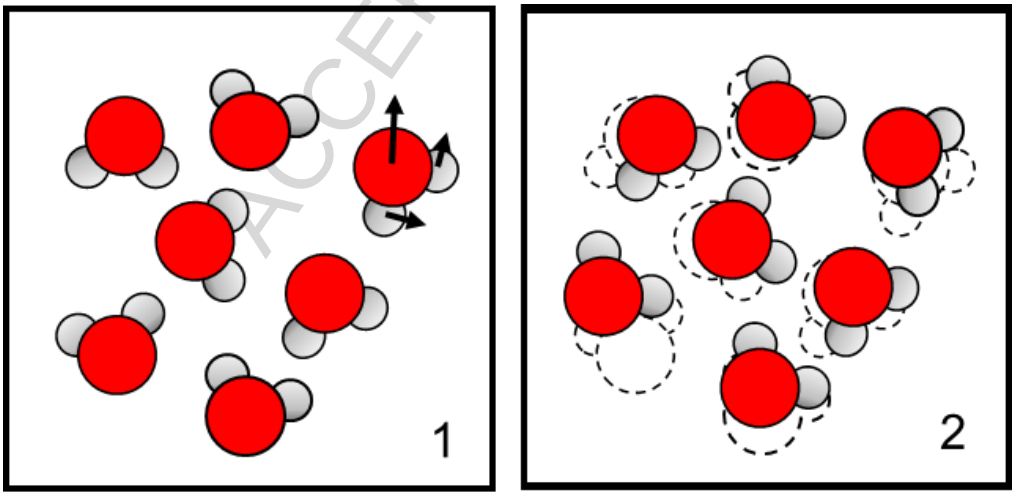

Figure 9. Molecular dynamics simulation. (1) The initial configuration comprising a set of atomic coordinates is specified and the atoms are assigned a set of random velocities that are consistent with the temperature of the simulation. The total force resulting from the interaction with all neighbouring atoms is calculated. (2) The new position of each atom at a very short time interval in the future ($\Delta t \sim 10^{-15}$ s) is calculated using Newtonian mechanics (Equation 29) from a knowledge of the force on each atom, its current velocity and its mass. The particles are then displaced to the new set coordinates. This process of

evolving the system one step at a time into the future is then iterated millions of time to yield a trajectory of the molecular behavour as a function of time.

Other than the time scale limitation, the other two primary limitations are the number of molecules in the system, and the accuracy of the force field parameters that characterize the intermolecular interactions. The molecular system size is typically of the order of 100,000 particles in a volume element of about a 10 x 10 x 10 nm^3, which is well away from cm-sized samples in the laboratory and Avagadro's number. The simulations do however employ periodic boundaries, which give periodicity to the system as benefits a crystal. The force fields are improving continually; the current level of accuracy has yielded some success in crystal structure prediction (given a 2-D molecular structure), which is a remarkable feat (see Section 5.1) [92-94].

An alternative to molecular dynamics simulations is the method of Monte Carlo (MC) simulation [23]. Instead of tracking a trajectory as a function of time, MC is implemented as a set of random moves, typically displacements of atoms and deformations of the simulation cell. New molecular configurations are accepted/rejected on the basis of their difference in potential energy ΔE. The imposed probability for accepting a trail displacement or cell deformation move is:

$$p_{accept}^{MC\ move} = \min\left\{1, \exp\left[-\frac{\Delta E}{k_B T}\right]\right\} \qquad -(30)$$

Simulations can be carried out in a variety of ensembles including *NpT*. The method yields equilibrium structures (hence phase stability) and thermodynamic quantities. A particular advantage of MC is that one can utilize non-physical moves, which can be useful for enhancing ergodicity (overcoming barriers) within the system. Clearly, if there is no reference to time, MC contains no information on dynamical processes. Kinetic Monte-Carlo however reintroduces time by attributing a characteristic time scale to each type of Monte-Carlo move. It usually requires experimental data or molecular dynamics simulations to assess the average time scales of the underlying processes (diffusion moves, rotation, etc.)

4.2 Simulating phase transitions

Among the first breakthroughs in simulating solid-solid phase transformations using molecular dynamics simulations was the pioneering work of Parrinello and Rahman [95,96]. As indicated above, molecular simulations of crystals invariably employ periodic boundaries to model a bulk system without surfaces. These periodic boundaries can restrain and limit solid-solid phase transitions in crystals that involve significant changes in the lattice. The boundary effects become less significant as the simulation cell (system size) is increased. The Parrinello-Rahman algorithm allows the simulation cell to change volume *and* shape in response to the difference in the internal stress of the system and the set pressure. The change in shape facilitates the transformation of a lattice of the initial phase with a particular symmetry and space group into another.

Where the energy barriers to transformation are much larger than k_BT, setting up the model system in a standard (brute force) MD simulation and waiting for the transition to happen spontaneously during the limited time scales (nano- to micro-seconds) of the simulation is unlikely to yield success. An intuitive way to promote the kinetics of phase transformations, with a view to observing the transformations in an MD simulation, is to apply enhanced pressure, superheating or supercooling. In the laboratory, moderate increases in any such driving force can be employed to enable phase transformations to within time scales of seconds to hours. In molecular dynamics simulations, the increase of thermodynamic driving however needs to be dramatically larger. First, the accessible time scales (nano- to micro-seconds) are at least six orders of magnitudes lower. An additional issue is that the typical system size is considerably smaller. Nucleation events occurring at some location within cm-sized samples in the laboratory, need to manifest within nm-sized systems in the computer simulation. For this reason, the state-of-the-art in molecular simulations for investigating phase transformations refers to technical strategies that – in one way or the other – *coerce* or *direct* the system to transform and then try to correct for the biasing. Whilst the system is forced to transform from one phase to another, the actual pathway and mechanism by which the transformation proceeds is (largely – see discussion below) unbiased, which represents the new information. Additionally, these techniques yield the free energy barriers to transformation – the key quantities that define the kinetics.

Directed simulations implement artificial forces or steered molecular displacements to induce the process of interest. The simplest implementation is to define (on the basis of intuition or insight) a model reaction coordinate R_C and then constrain the system to move the along this coordinate whilst allowing all other degrees of freedom to relax. For a phase transition, the reaction coordinate would be the transformation pathway or mechanism by which the parent phase transforms to the new phase, which may for instance take the form of an order parameter for investigating the nucleation step. A series of simulations are carried out with the model structures constrained at particular points of the reaction coordinates (particular values of the order parameter for the case of nucleation) whilst monitoring the constraint forces. From the constraint forces one can calculate the free energy profile, often termed the potential of mean force, as a function of the model reaction coordinate (Figure 10) including the free energy barriers characterizing the phase transformation process. A variation on this approach is the method of *umbrella sampling*. Rather than simulating the system constrained at various points on the reaction coordinate, the system is instead *restrained* at the particular points on the reaction coordinate using forces derived from artificial harmonic potentials $U(R_C)$ (Figure 10). The tendency of the system to depart from the restrained positions is monitored yielding a probability histogram of occurrence $h(R_C)$. A strong tendency for the system to depart from a particular restrained position reflects an unfavourable (high energy) position on the free energy profile characterising the reaction coordinate. Using Boltzmann statistics, the occurrence histogram may related to the corresponding free energy profile, the potential-of-mean-force pmf(R_C)

$$\mathrm{pmf}\left(R_C\right) = k_B T \cdot \ln\left[\frac{h\left(R_C\right)}{h_0}\right] - U\left(R_C\right) \qquad -(31)$$

In the case of low energy barriers, straight-forward molecular dynamics or Monte-Carlo simulations can provide the full occurrence histogram $h(R_C)$ without the use of artificial potentials $U(R_C)$. The quality of directed simulation methods depends critically on the choice of the model reaction coordinate. For complex processes, defining an appropriate reaction coordinate may be challenging.

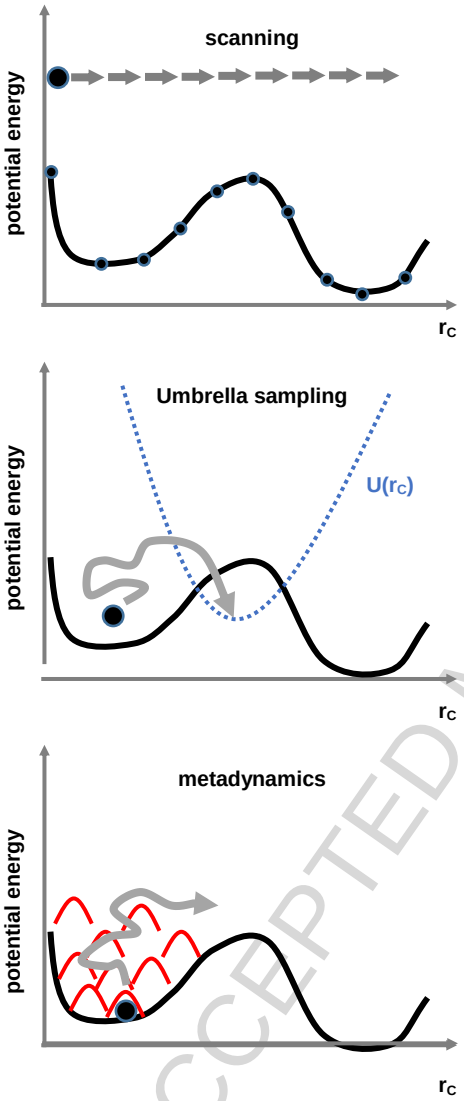

Figure 10. Illustration of energy profile calculations from molecular simulation. Top: potential energy is scanned as a function of the model reaction coordinate. Middle: boosting free energy calculations from enhanced sampling of occurrence profiles using attractive potentials. Bottom: escaping energy minima from metadynamics using locally repulsive potentials.

Clearly, un-directed simulation methods are preferable, being free from errors resulting from either a biased or an ill- pre-defined reaction coordinate. The increasingly popular *metadynamics* approach [97,98] accelerates the phase transformation process by filling-in and swamping (on the fly) the full spectrum of local minima in the free energy surface, thus raising and leveling the energy surface and enabling the system to negotiate the energy barriers more readily, undirected. The minima swamping is tracked, from which the free energy profile i.e. the barriers to transformation, may be reconstructed. Metadynamics thus utilises bias potentials akin to umbrella sampling, but relies on repulsive potentials $G(rC)$ to disfavor configurations that occur particularly frequently. This has the great advantage in that the system moves away from configurations of the reaction coordinate that have already been explored, whilst allowing it to sample alternative configurations *without directional forces* (other than disfavoring the already known structures). A simulation started from a relaxed structure may thus escape local energy minima by iteratively adding repulsive potentials until the effective barrier to reaching a new energy minimum can be surmounted (Figure 10). Convergence is reached after filling of all local energy minima, thus resulting in a flat histogram for the sampling of the reaction coordinate. The potential of mean force that reflects the free energy barriers can be reconstructed from the tracked, added repulsive potentials.

The appealing efficiency of metadynamics allows scanning of free energy profiles as functions of several descriptors, named collective coordinates. The significance is that the reaction coordinate i.e. the molecular pathway by which the transformation is observed to proceed, becomes less biased by our choice of collective variable(s) as the number of collective variables increases. The reaction coordinate is then deduced from the minimum energy path sampled for this set of variables. The current state-of-the-art is to sample coordinate space in up to 6-dimensions; however, in many cases mechanistic insights of high quality can already be obtained from 2-3 adequately chosen descriptor variables.

The effectiveness of the metadynamics for simulating phase transitions is illustrated by a study from Parrinello's laboratory where they to induced changes to the cell vectors of the crystals [99]. On this basis, free energy (and free enthalpy) landscapes were sampled as a function of the length of the cell vectors a, b, c and the respective angles α, β, γ – a total of 6 collective

coordinates. Screening different unit cell shapes and sizes in this way provided a route to polymorph screening. While computationally demanding, metadynamics simulations include entropic effects and convey significant further insights. First, metadynamics can explicitly be performed as a function of temperature thus providing temperature and pressure dependent polymorph search. Further, phase stability can be directly elucidated from respective minima in the free energy landscape [100]. Finally, mechanistic insights into the transformation process can be derived from the minimum energy path connecting the stable domains of the energy landscape. When moving the system in 6-dimensional coordinate space (a,b,c and α, β, γ), metadynamics shows the optimal molecular rearrangements for providing such unit cell distortion [101]. It is important that the simulation cell is a supercell comprising multiples of the unit cell (which then has periodic boundaries), which is more realistic as it can offer insight into phase interface formation, a prominent example being the observation of stacking faults as intermediates in the high-pressure transformation of $MgSiO_3$ minerals [102]. A simulation comprising a single unit cell is akin to implementing a second order phase transition, that is collective molecular displacements throughout the bulk crystal – whatever happens in the single unit-cell simulation box is simultaneously reproduced in all the periodic images.

Biasing is pretty much eliminated in *transition path sampling* (TPS) simulations [103,104]. Here we sample an ensemble of system trajectories between the starting state (in the present context, the parent crystal) and the final state (the new daughter phase), and identify the low-energy barrier (hence the most probable) pathways. This method can be seen as a Monte-Carlo iteration of sampling dynamic transition pathways. While the starting molecular configurations may be strongly biased (selected perhaps from a biased simulation), the nature of Monte-Carlo moves in trajectory space results in evolution to low-energy pathways, i.e. unbiased convergence to the most favorable transition route. Given an initial configuration lying close to the transition state regime (that is, the manifold of all possible transition states), molecular dynamics simulations are performed in both directions of time i.e. forwards to generate the new phase, and backwards to yield the parent crystal. This constitutes a single trajectory linking the two states. To explore further routes, configurations of the previous trajectory are slightly modified and the process repeated. To confine trajectory space sampling to transition routes only, pathways that do not connect the desired endpoints (starting and final phase) of the (transformation) process are

discarded. Within a few tens of such iterations, the observed pathways typically converge to the favorable transition mechanism (Figure 11). In other terms, the arbitrarily chosen transition state of the initial pathway is optimized in favor of the energetically most preferred transition state. Moreover, by comparing the likelihood of trajectory propagation to the desired endpoints it is possible to calculate forward (r→) and backwards (r←) reaction rates. This can be done for a series of intervals *i* of the descriptor variable, thus providing a reaction flux profile. The free energy difference between these intervals may then be estimated from the ratio of forward and backward rates using Boltzmann statistics.

$$\Delta pmf\left(i \to i+1\right) = -k_B T \cdot \ln\left[\frac{r_{\rightarrow}\left(i \to i+1\right)}{r \leftarrow \left(i+1 \to i\right)}\right] \qquad -(32)$$

Transition path sampling was first applied some 15 years ago to simulate pressure-induced phase transitions [105]. While typically starting from artificial transformation pathways (such as collective unit cell distortion), the iterative sampling of transformation pathways in TPS was found to quickly evolve in favor of low-cost routes. Upon convergence, these pathways all reflected the same overall mechanism, but differed in terms of where the nucleation started.

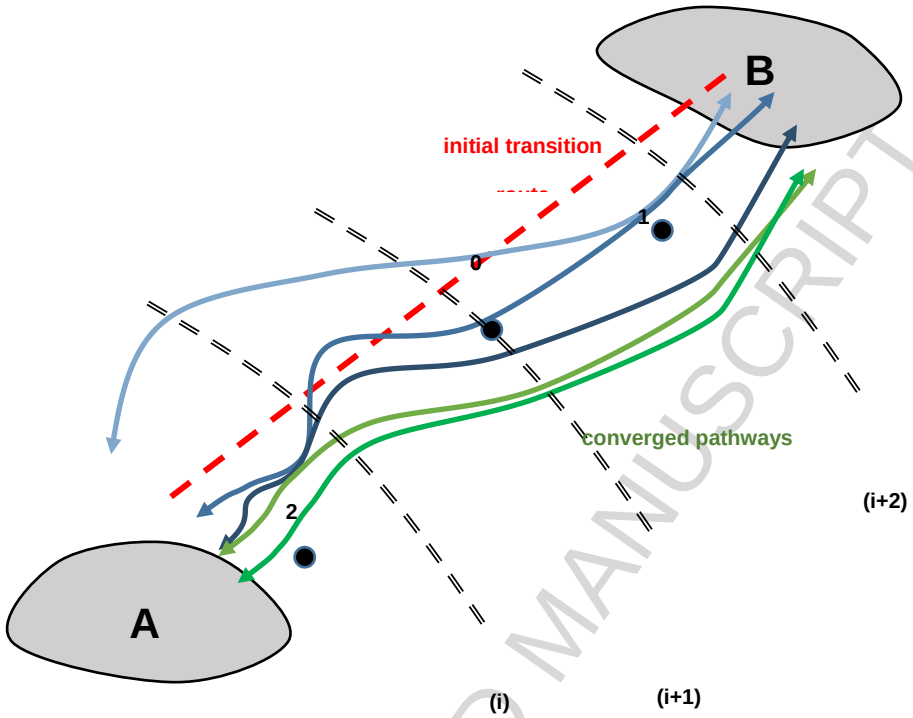

Figure 11. Illustration of transition path sampling between two phases A and B. The initial route is derived from simple geometric interpolation (red dashed line). Subsequent Monte-Carlo moves (indicated by numbers 0,1,2) in trajectory space lead to new pathways (blue curves). Upon sufficient iterations the pathways converge to the favored mechanistic route, represented by a bundle of similar trajectories (green curves). For rate calculations, it is useful to devise pathways in intervals of milestones, each reflecting a transition interface (i) in trajectory space.

The performance of either of these (un-)directed methods, metadynamics or transition path sampling, depends on the system and the actual process of interest. Based on our personal experience, metadynamics is suggested if the key descriptor variables appear safe to guess. The (more expensive) transition path sampling approach (and its derivatives like transition interface

sampling and aimless shooting) is appropriate in case of complex processes with larger likelihood of showing unexpected mechanistic routes. Examples for both cases are discussed in the following section.

5 Molecular simulations of phase stability and transitions

5.1 Crystal structure prediction and polymorph screening

Being able to predict the crystal structure of a chemical compound given only its molecular structure has been a fundamental challenge in computational chemistry [106-108]. Having such an ability to would enable prediction and rational design of a whole variety of solid forms including polymorphs, solvates, co-crystals and salt forms. It would open the door to the more significant goal of predicting material properties such as mechanical properties, solubility, dissolution, and surface and interfacial energies using a minimum of *a-priori* information. Such methodology could form the basis of an in-silico screen to identify molecules and associated solid forms with optimal properties without synthesizing the pool of potential compounds. A particularly important application is solid form screening to identify potential forms that may show up either during processing or on storage - which is crucial not only for selecting favorable candidates, but also to avoid undesirable forms.

There has been considerable progress in both methods and protocols, reflected with some successes, for crystal structure prediction of organic molecules. Whilst there are a variety of proposed methods for predicting the crystal structure, most of them comprise 3 distinct steps:

(i) Exploration of conformational flexibility of the molecule, usually involving quantum chemistry codes to ascertain and characterize the barriers to rotation about bonds;

(ii) Generation of tentative crystal packings for the molecule, the common approaches being either random or pseudo-random exploration of phase space (lattice parameters, molecule position and orientation and internal degrees of freedom) and simulated annealing.

(iii) Ranking of the trial crystal structures in terms of potential energy, the lowest energy structures being considered to be the most plausible. The rigorous criterion, of course, is free energy but this is demanding to evaluate in terms of computing resource. The

neglect of entropy implies the potential energy criterion to be a 0 K approximation. Initial screening of the large number (1000s) of trial structures is commonly carried out using the computationally efficient (but lower accuracy) molecular mechanics forcefields to yield a short list of plausible structures. The latter are then ranked using quantum chemistry codes, typically density function theory (DFT) with dispersion interaction corrections.

The capability of the computational chemistry community to predict crystal structures has been regularly tested by 'blind tests', which have served to identify the truly effective approaches from the competing claims made in the literature. The 6th blind test was launched in 2014 with the results being reported in 2016 [94]. Within this blind test, all of the experimental crystal structures of the five targets (rigid molecule; partially flexible molecule; partially flexible salt form; multiple partially flexible molecules forming co-crystal or solvate; large flexible molecule) were predicted by one or more of the submission. In terms of methodology, the success stories are the methodologies of Neumann, Leusen and Kendrick [92], and of Price et al [109]. The Neumann methodology is implemented in the code *Grace®*, which is marketed by Avant-garde Materials Simulation. *Grace* is being used in the pharmaceutical industry for polymorph prediction. A recent contribution of Nyman and Day [110] indicates that entropy contribution (which was calculated using lattice dynamics) is important in ranking of polymorph stability.

Clearly, in simulating phases and phase transitions, the accuracy of the force field parameters is key. An accurate forcefield should be able to preserve the crystalline phase structure at a given temperature and pressure. A significant deviation (>5%) in the crystal structure and lattice parameters implies an inadequate force field. Should the latter be the case, one should consider alternative set of forcefield parameters or optimize the parameters to reproduce the known crystal structures and their lattice energies [111-113].

The blind tests and broader crystal structure prediction studies reveal the current accuracy of molecular mechanics force fields in this context to be comparable or just beyond the small differences in lattices energies of the polymorphic forms, circa 0.2-2 kJ mol^{-1}. Hence, the need to resort to quantum chemistry methods to re-rank the final short list of structures as obtained from force-fields.

5.2 Coexistence and phase diagrams

Crystal structure prediction methods are based on identifying structures with minimum potential energy and typically do not include entropic effects. Such an approach therefore cannot predict the phase diagram of a material as a function of temperature. At phase coexistence, the chemical potential of the phases concerned is identical. For a pure system, the chemical potential is given by

$$\mu = \left(\frac{\partial G}{\partial N} \right)_{p,T} \quad -(33)$$

which expresses the affinity of a molecule to be within the given system.

Hence, *free energy calculations* are required to predict phase diagrams. There are three main approaches to predicting phase diagrams: lattice dynamics [114]; thermodynamic integration/perturbation using an Einstein crystal [115,116] coupled with Gibbs Duhem integration [117]; and (iii) density of states methods [118](112). Applications of the latter have so far been restricted to very simple systems.

For solids, the number of configurations is limited and direction integration of the partition function becomes feasible, which forms the basis for lattice dynamics. The method involves calculation of the vibrational and librational modes of motion of the molecules in the crystal lattice in the harmonic approximation using the intermolecular forces. The coupled vibrational motion of the molecules is transformed into independent harmonic oscillators using normal mode analysis to yield a phonon density of states, which enables the calculation of the free energy of the solid via the partition function. The harmonic approximation appears to be valid up to about two-thirds of the melting temperature of the crystal. Applications of lattice dynamics to predict phase diagrams include MnO forms as a function of pressure [119], DL-norleucine as a function of temperature [111], and methane gas hydrate as a function of pressure [120].

The Einstein crystal approach coupled with Gibbs-Duhem is more elegant than lattice dynamics, and in principle more accurate at any temperature. It is however more demanding in terms of computing resource. There are two stages: the determination of a coexistence point on the phase diagram using the Einstein crystal approach, and (given a co-existence point) the tracing of the phase diagram by integrating the Classius-Clapyron equation. The Einstein crystal approach

links reversibly an ideal (non-interacting) system to the real lattice. The free energy of the ideal Einstein crystal is calculated analytically and the change in free energy from the ideal to the real crystal is determined by molecular simulation using thermodynamic integration, the total free energy for the crystal being given by the sum of the two. Notable applications include the prediction of the phase diagram of water [121] – a tour de force (see Figure 12), and the melting point of NaCl [116].

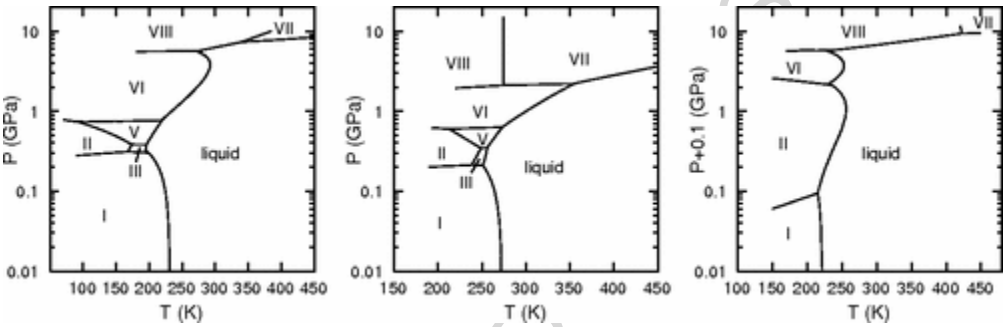

Figure 12. Predicted (for TIP4P model of water; left) and experimentally determined (right) phase diagrams of water. Only the stable phases of ice are included in the diagrams. (Reproduced with permission from reference [121] E. Sanz, C. Vega, J. L. F. Abascal, and L. G. MacDowell, Phys. Rev. Lett. 2004, 92, 255701; copyright 2004 American Physical Society).

5.3 Displacive/martensitic transformations

The seminal work of Parrinello and Rahman [95,96] – enhancement of the MD simulation method to enable the simulation cell to respond to internal shear stresses – opened the way to simulating crystal-crystal phase transitions. Their studies on simple ionic systems were immediately followed by what were then considered to be large scale simulations (typically 2048 molecules) on molecular crystals that included SF_6 [122] and n-butane [123,124] using the massively parallel ICL Digital Array Processor (DAP) computer. It is notable that these simulations were of phase transitions between plastic phases, involving relatively small molecular displacements and low transition barriers i.e. displacive transformations in Buerger's language.

The primary macroscopic characteristic of martensitic transformations is that they exhibit displacive shear upon transformation giving rise to shape-change in the material. The other often

stated characteristics are a transition velocity being of the order of speed of sound, and diffusionless, cooperative motion of the atoms/molecules. It is interesting to consider as to what exactly needs to occur in terms of mechanism to give rise to macroscopic shape-change that can result in the crystal doing external work? Uncoordinated molecular displacements lead to a cancelling-out of any net motion or net force that could result in a specific deformation. A specific deformation of the material must therefore result from synchronized, collective molecular displacements. Collective molecular displacements imply that the energy barrier for a particular (or a few select) transition pathways – the particular collective molecular displacements – is significantly lower than all other potential pathways and outcomes. A topotaxial relationship between the initial and the final lattice would suggest that a few select mechanism pathways are favoured, and hence may represent a characteristic feature of martensitic transitions. It is therefore clear that the nature of the molecular displacements during a phase transition is at the heart of understanding martensitic transformations.

Martensitic transformations, as indicated above (Section 3.1), have significant technological applications, though these are currently largely restricted to metals, alloys and ceramics, A particularly exciting prospect is the possibility of exploiting such transformations in molecular crystals to develop tiny machines for biomedical use, for instance, to target and deliver genes or drugs. An extraordinary example of one such nature's machine is the T4 bacteriophage virus. This virus employs a martensitic transformation of its sheath protein to puncture the bacterial membrane to enable it to deliver its DNA content [125,126]. Converting chemical energy into mechanical activity is the essence of a machine. A greater molecular-level understanding of thermosalient molecular crystals [15,57] (often referred to as 'jumping crystals') could set the foundation for developing tiny machines based on organic molecules.

For molecular crystals, mechanistic insight into martensitic-type transformations has come from simulations of phase transitions in crystals of DL-norleucine [111,127-130] and terephthalic acid [131]. The three known forms of DL-norleucine consist of stacked, hydrogen-bonded bilayers, separated by a van der Waals surface. Simulations on the $\beta \rightarrow \alpha'$ (α' being a variant of the experimentally observed α phase) transition in DL-norleucine reveal a remarkable wholesale shifting (a synchronized displacement of all the molecules within a bilayer) of the molecular bilayers relative to each other (see Figure 13). There appeared to be no nucleation event or local

hot spot at which the transformation is initiated. Effects of vacancy defects was also investigated but again the transformation proceeded by concerted molecular displacements. An often quoted argument against collective motion in phase transitions is that the overall barrier is extensive (thermodynamic definition), i.e. depends on the number of molecules involved in the collective motion [27]. If the activation barrier for a single molecule is $G^{\ddagger}$, then for the collective motion of a layer of n molecules,the overall barrier would be $nG^{\ddagger}$. The implication is that the barrier will become insurmountable even for a relatively small number of molecules engaged in collective motion. And yet the DL-norleucine simulations reveal concerted motion over hundreds of molecules, indeed along at least the full 10 nm dimension of the simulation cell.

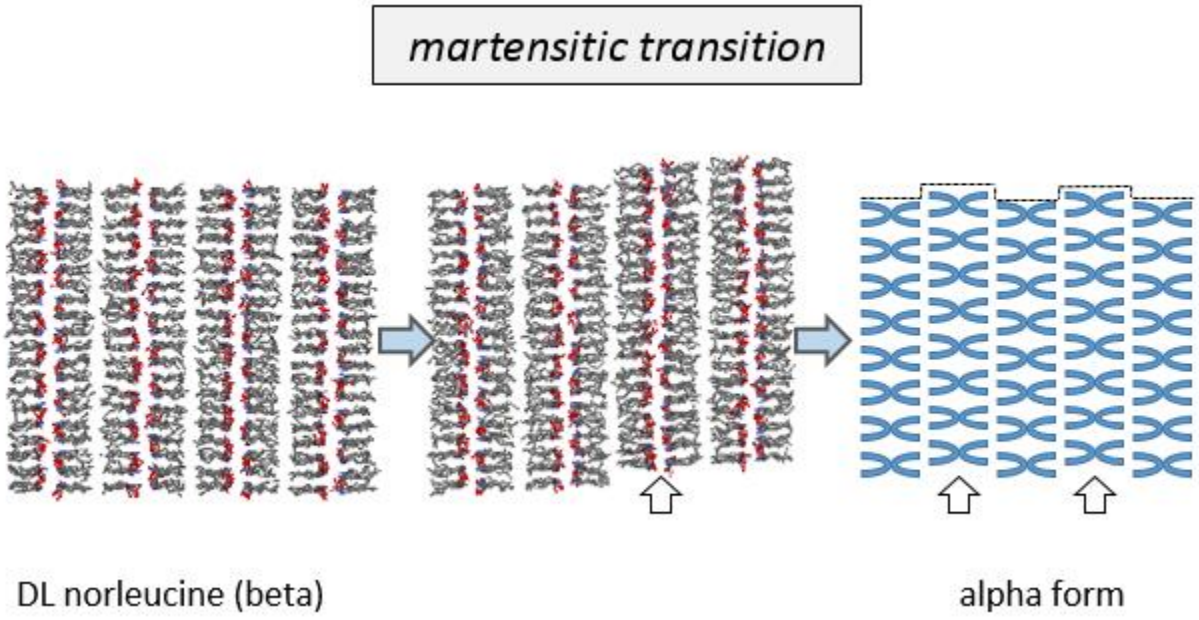

Figure 13. Illustration of a periodic simulation cell of DL norleucine. Left: beta (low-temperature) form characterized by hydrogen bonded layers (H-bond donors and acceptors are shown as blue and red balls, respectively). Center-to-right: upon heating adjacent layers that interact via comparably weak van-der-Waals forces can shift (white arrows) leading to the alpha form (right). Note that within the layers the molecules move in a quite concerted manner thus apparently skipping nucleation and growth. (Reproduced with permission from reference [128] D. Zahn & J. Anwar, Chem Euro. J. 2011, 17, 11186-11192; copyright 2011 Wiley-VCH Verlag 11186 GmbH).

The first DL_norleucine simulations were carried out by standard brute force MD and employed what could be considered as rather high superheating to induce the transformation. The apparent observed collective motion may not reflect the mechanism closer to co-existence which would be more relevant to real world applications. In view of this the DL-norleucine transformation was further investigated using the unbiased transition path sampling approach [129]. The TPS method was combined with quenching of the system energy during the trajectory simulations, which enabled the identification of the single low-barrier pathway. This pathway too was characterized by a wholesale shifting of the integrated bilayers, as observed in the brute force MD. These results are atypical in that such TPS simulations on other systems have invariably revealed a nucleation and growth mechanism. For DL-norleucine, the process appears to involve a compression wave but with a wavelength beyond the 10 nm scale of the simulation cell. The transition energy barrier was not found to be extensive i.e. not dependent on the number of molecules involved in the collective motion. The argument for the energy barrier to collective motion being extensive presumes that the shear at the interface occurs as a result of an applied stress. In this respect i.e. an externally applied stress, the argument is expected to be valid. However, with thermally induced transformations, the thermal energy is *distributed* across all degrees of freedom, and individual molecules would have an independent capacity to mount the local barrier. The analogy given in support of an extensive barrier is the increasing difficulty one encounters in attempting to pull a carpet across a room as the carpet area increases. For a thermally-induced transformation, staying with the carpet analogy, the thermal energy acts as an anti-gravity potential (on each and every molecule) at every point on the carpet, enabling the carpet to glide into another preferred location (another minimum). With the carpet, an alternative low-cost approach to displacement is to introduce a local kink and then to push that from one end to another. This is akin to the compression wave observed in the DL-norleucine transformation.

Terephthalic acid crystals apparently release mechanical energy during the form I to form II transformation that can cause the crystals to jump, suggesting a martensitic-type transformation [132]. Beckham et al [131] investigated this transition by molecular simulation using the technique of aimless shooting, a variant of transition path sampling. Notably, these simulations were carried out on *nanocrystals* of terephthalic acid rather than bulk crystals, which enabled the possibility of crystallite shape change and associated release of mechanical energy to be explored (Figure 14). The TPS simulations yielded the transformation pathway, which was validated using

committer probability analysis. In this case, the transformation reveals a nucleation and growth mechanism, with nucleation being initiated at the surface. The nuclei were elongated which appears to be reasonable given that the 1-d hydrogen binding between the carboxylic groups yields integrated chains. The transformation velocity along the predicted edge was estimated to be approximately 8 m/s equating to a kinetic energy of about 0.3 kcal/mol, which was considered sufficient to induce jumping of the crystal.

The study investigated two nanocrystal models of identical shape but with different total number of terephtalic molecules (343 and 216). For these two models, umbrella sampling simulations showed free energy differences ΔG between the two polymorphs of 10 and 3 kcal/mol, respectively. Thus, by reducing crystal size from 343 to 216 molecules, ΔG does not scale linearly, which would imply about 6 kcal/mol for the N = 216 molecules model. This discrepancy illustrates the importance of local nucleation and growth phenomena – here initiated at the crystal surface – for characterizing polymorphic transitions.

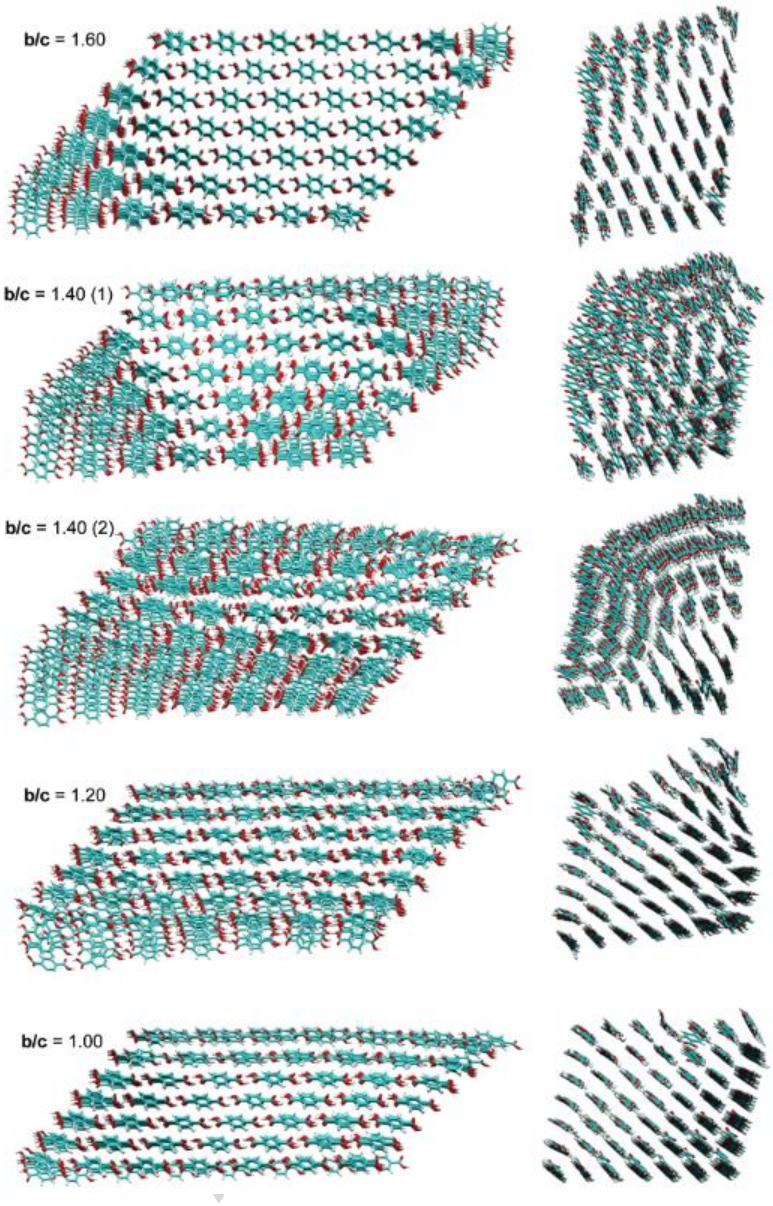

Figure 14. Snapshots from the polymorphic transition of a terephalic acid crystal comprising 343 molecules shown along the [010] (left column) and [100] (right) direction, respectively. Nucleation starts at the crystallites corner (snapshot at the top left) and the progress of the transformation is monitored by the change of b/c aspect ratio from 1.6 to 1. (Reproduced with permission from reference [131] G. T. Beckham et al. J. Am. Chem. Soc., 2007, 129, 4714–4723; copyright 2007 American Chemical Society).

5.4 Reconstructive transformations

In contrast to displacive transformations, reconstructive transformations are considered to be characterised by strong interactions with little or no structural relationship between the parent and the new phase. Whilst the strength of the interactions can affect kinetic stability and material hardness at ambient conditions, putting different materials on a reduced temperature scale ($T/T_{\text{melting point}}$) reveals that classifying transformations on the basis of the strength of interactions is rather arbitrary. The underlying physics of transformations in hard and soft materials may be similar.

Hard and brittle compounds such as ionic crystals strongly disfavor lattice distortions and during a transformation tend to show sharp phase interfaces at which bonds are broken and reformed [59]. In other terms, such reconstructive transformations provide comparably low strain within the phase domains at the cost of relatively high interface energy. For instance, reconstructive transitions were observed for the pressure-induced *B1–B2* transformation in alkali halides [60,133] (Figure 15). For these compounds transition-path sampling molecular dynamics simulations revealed that nucleation starts with the displacement of a single ion, followed by shifting of an entire column. Phase growth was identified as the parallel shifting of adjacent columns in one direction, whilst anti-parallel shuffling of layers occurred in the perpendicular direction. The local nature of such nucleation events allowed the observation of independent nucleation events separated by distances within the nm scale. Thus, sufficiently large simulation models can capture coexisting nuclei and allow the investigation of phase domain coalescence, competing growth or merging by grain boundary formation. For a 14×14×14 supercell model of RbBr, the different senses of column-wise shuffling along the (initially) equivalent a, b and c direction of the parent lattice lead to ‘mismatching’ nuclei that, upon contact of the phase fronts, yielded a poly-crystalline structure comprising grains, even though the original structure was a coherent single crystal [60].

It is interesting to compare the transformation of alkali halides with that of the somewhat softer and less brittle semiconductor CdSe [59]. For the latter material, more extended interface regions separating the parent and high-pressure phases were observed. In other terms, more elastic compounds may accommodate phase interfaces in a structurally more continuous manner and thus avoid harsh interface energy by some degree of elastic smoothening. Such elastic

deformations in turn imply longer-ranged stress emitted by the phase fronts, and thus prevent the formation of coexisting nuclei at short distance. Indeed, crystal fragmentation into grains could not be observed in the CdSe study and is instead believed to occur at by far longer length scales compared to the alkali halides [134].

Another notable transformation is that of graphite to diamond as a function of pressure. This has been reproduced by simulation using ab initio (brute force) molecular dynamics, although the required pressure was 90 GPa, which is 6 times larger than the experimental estimate of 15 GPa [135]. This large excess pressure is necessary to make the transformation occur within the relatively short timescales of simulation. In contrast, a metadynamics simulation using a tight-binding potential supplemented with a 2-body van der Waals interaction was able to induce the transformation close to the experimental transformation pressure [101].

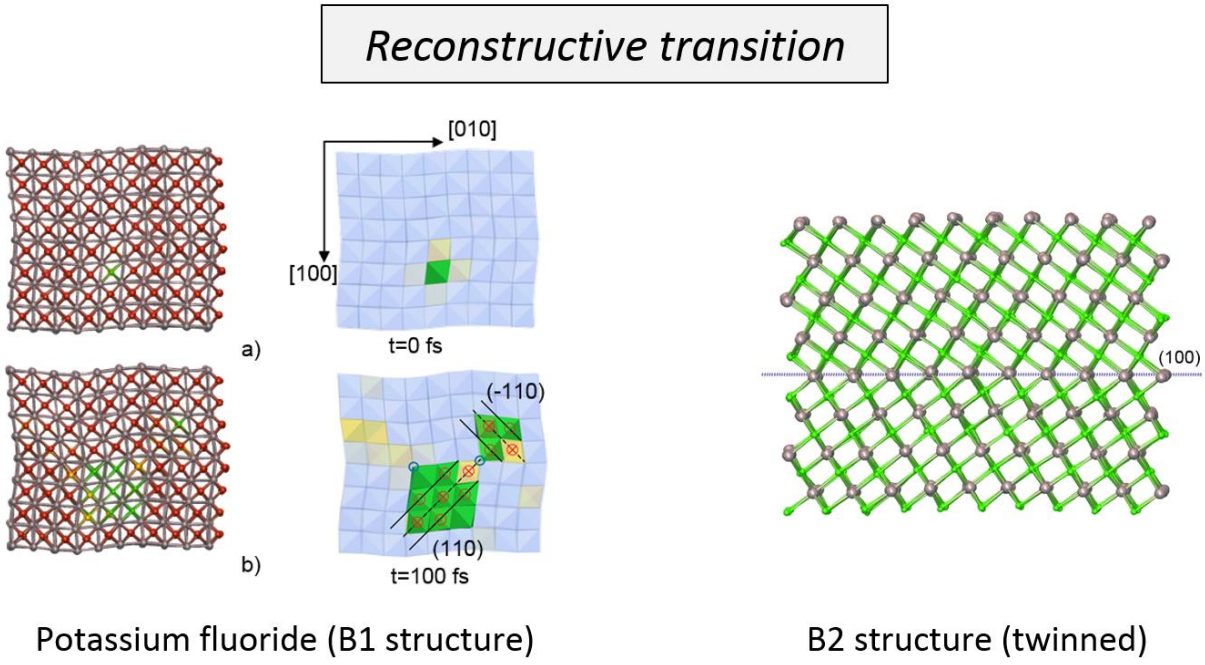

Figure 15. Reconstructive transition of KF involving a change in coordination number from 6 (*B1*) to 8 (*B2*). The change of coordination number is highlighted for the potassium ions using red (6), yellow (7) and green (8), respectively. The mechanism involves the shifting of adjacent ion columns along [100],[010] or [001], resulting in the up/down shuffling of layers as highlighed by plus and minus signs. The example shows two nuclei of the B2 phase which senses of (110) and (-110) layers mismatch. Upon contact of the two phase domains a grain boundary is formed (here in form of a twinning plane).

(Reproduced with permission from reference [126] D. Zahn, O. Hochrein, S. Leoni, Physical Review B 2005, 72, 094106; copyright 2005 American Physical Society).

5.5 Diffusive transitions

Diffusive transitions do not show a rigorous mapping of atomic displacements from one lattice to another, but instead involve a temporary degree of disorder. There are examples of polymorphic transitions in molecular crystals induced by high temperature that follow the scheme phase I → melting → phase II type transformations or are solvent-mediated phase transitions, i.e. dissolution and re-crystallization. These exceed the scope of the present review. Interestingly, the temporary disorder may be limited to a specific constituent of a multinary solid, as for example observed for ion conductors [73].

5.6 Effects of defects

While mechanisms of polymorphic transitions are often discussed on the basis of perfect single crystals, we should bear in mind that such models ignore possibly quite important features of real crystals. It is intuitive to expect defects to locally affect the energy barrier to nucleation (and phase propagation). Simulation work exploring this issue is still rare. An illustrative example is the *B1–B4* pressure-induced transition of GaN [136]. Transition path sampling simulations allowed the transition to be simulated without drastic over-pressurization, providing the basis for observing even subtle changes in the nucleation mechanisms upon defect incorporation. Substituting gallium (Ga) by more polarizable indium (In) atoms leads to preferential nucleation near the defects, whilst substitution by harder aluminium (Al) atoms was demonstrated to hinder B4 nucleation. Using more than 5% Ga → Al substitution even altered phase stability in favor of the high-pressure form.

The second example is that of the pressure-induced *B1*(*Fm3m*)–*B2*(*Pm3m*) transformation in KCl. This transformation is rapid and reversible, occurring at 1.9 GPa but exhibits hysteresis that depends on purity and history of the sample. The effects of vacancy defects (both quantity and distribution) were investigated using molecular dynamics simulation at high pressures [137]. Nucleation always occurred at the vacancy defect sites and hysteresis was reduced with increase in density of defects. The transition pressure observed in simulations of perfect crystals was

about 7 GPa which dropped to about 2.5 GPa on introduction of the vacancies, just 0.6 above the experimental transition pressure.

5.7 Phase stability and transitions at the nanoscale

Going down the length scales gives rise to some new physics. As a crystal decreases in size, its surface or interfacial free energy (the choice depends on whether the crystal is stand alone or surrounded by some medium) becomes significant relative to its bulk free energy and the thermodynamics of the crystal are now determined by the interplay of these two energies. For polymorphs, the molecular organization at the crystal surfaces is likely to be different and so would the surface energies. Therefore, depending on the crystal size, the surface (interfacial) energy can favour a particular phase that otherwise may be unstable in the bulk or even an entirely new phase, hence enabling phase stability to be modulated at the nanoscale.

Particle-size dependent phase stability was first recognized for inorganics, specifically metal oxides [138]. Of the various polymorphs of TiO2, rutile was found to be the stable phase in coarse materials, whilst the anatase and brookite were commonly observed in nanosized samples. These observations were rationalized by surface energy measurements to yield phase diagrams comprising enthalpy as a function surface area (particle size), which revealed cross overs in stability below about 200 nm [139,140]. The oxides ZrO_2 [141] and Al_2O_3 [142] also exhibit similar particle size-dependent phase stability, as does carbon for which nanodiamonds are more stable than graphite [143]. Molecular simulations have played a key role in predicting phase stability switch-overs for these inorganic oxides and in rationalizing observed experimental data, for example, see surface energy calculations on Al_2O_3 [144].

In contrast to inorganic oxides, there appears to be little or no experimental data on phase stability of *stand-alone* organic nanocrystals. This is not surprising since it is pretty much impossible to generate stable stand-alone nanocrystals of organics, given that they are relatively soft compared with metal oxides. Simulation studies are also sparse. A notable contribution is that of Hammond and colleagues [145], who investigated the potential energy of the two known forms of L-glutamic acid nanocrystals as function of crystal size. The calculations suggest that the metastable α-form is more stable than that β-form (which is the stable form in the bulk) for small particle sizes. Using potential energy implies a 0 K model with the entropic effects being ignored. An enhancement would be to carry out free energy calculations, which are now feasible.

As yet there is no experimental verification of the predicted switch-over in phase stability for L-Glutamic acid polymorphs.

Whilst preparation of stand-alone, organic nanocrystals is challenging, nanocrystals can be crystallized under nanoscale confinement in nanoporous matrices [146, and references therein]. As would be expected, there are many examples where the confined nanocrystals exhibit striking departure in phase stability from that in bulk crystals. Notable examples include glycine [147], paracetomol [148], and 5-methyl-2-[(2-nitrophenyl)- amino]-3-thiophenecarbonitrile (often referred to as ROY due to the red, orange and yellow colors of its various polymorphs)[149]. In confined systems, the important quantity is the interfacial energy rather than surface energy, which would depend on the nature of the confining surface and hence in principle could lend to being modulated by design.

A recent study by Belenguer et al [150] investigated solvent effects on phase stability at the nanoscale experimentally on grinding complimented by interfacial energy calculations using density functional theory. They were able to demonstrate phase stability switch-over as a function of size for the molecular systems studied.

At the nanoscale, other than the potential for switch-over of phase stability (thermodynamics), the barriers to phase transitions (kinetics) can also be modulated. The transition state theory indicates that, of the ensemble of phase transition pathways that are available to a system, the ones explored by the system are those with the lowest free-energy barrier. For nanocrystals (nanosystems in general), as the overall free energy is composed of both a surface (or interfacial) and a bulk component, the important pathways will be those with the lowest *surface free-energy barrier*. The significance is that for nanocrystals, given that phase transitions from one phase to another will invariably involve some local or global lattice expansion, the free energy barriers associated with any required increase in *surface* could be significant. Consequently, kinetics may have a stronger role in determining phase stability of nanocrystals than previously recognized.

The role of the surface in modulating the barriers to phase transition was recognized in simulations carried out on both bulk crystals and nanocrystals of DL-norleucine [128]. In the simulations, the $\beta \rightarrow \alpha'$ transformation in bulk crystals (with periodic boundaries) is observed at about 390 K. For the nanocrystal (dimensions of approximately 12 x 10 x 10 nm), the β-phase remained stable until 470 K, above which the nanocrystal transformed to another phase

altogether. From the above discussion, the lack of transformation could be either thermodynamics phase-stability switch-over or kinetic hindering. Thermodynamics could be discounted on the basis of the calculated potential energies of the nanocrystals of the two phases (the difference in entropy for the surfaces was considered to be minimal), implying kinetic hindering behind the lack of transformation. The role of the surface in enhancing barriers to transformation is illustrated schematically in Figure 16.

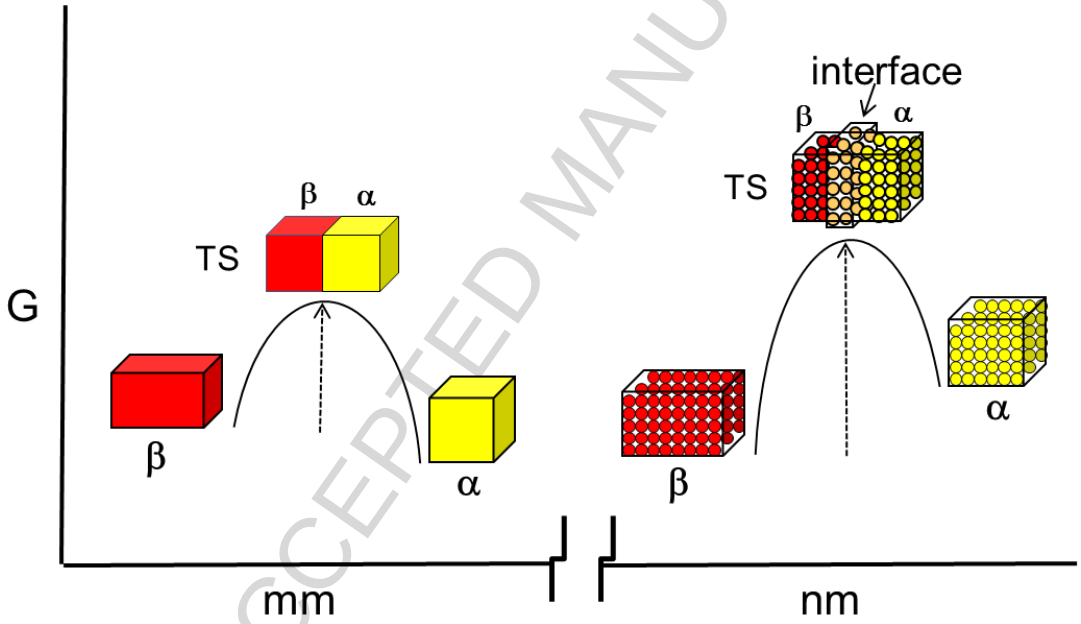

Figure 16. Polymorph phase stability and solid-solid phase transformations in bulk (mm) and nm-sized crystals. While surface effects are negligible in large crystals, at the nanoscale the surface energy can be significant and differences in surface structure between polymorphs can change the relative phase stability. Further, for nm-sized crystals, any local and/or global lattice expansion due to nucleation or interface development and advance could give rise to significant increase in the surface (and associated surface energy) of the particle, serving to increase the transformation barrier and leading to kinetic hindering. (Reproduced with permission from reference [128] D. Zahn & J. Anwar, Chem Euro. J. 2011, 17, 11186-11192; copyright 2011 Wiley-VCH Verlag 11186 GmbH).

Phase transformations at the nanoscale are also relevant at earliest stages of crystallization [128,151], where for example a system follows Ostwalds rule of stages [152,153] with the phase with the lowest energy barrier nucleating first. Size-dependent transformations were recently

observed in simulations of nucleation in DL-norleucine [151]. The simulations revealed alternative forms, micelles and bilayer segments, at the initial stages, presumably because these forms provide more favorable interfacial energy. These structures become unstable at large size in favour of a structure that begins to resemble the bulk periodic structure. The corresponding free energy profiles, illustrated by green and blue curves in Figure 17, hence represent local sketches of the minimum energy pathway to crystal formation. In-between, polymorphic transitions are induced by size-dependent phase stability, but also confined by size-dependent barriers. To contrast such structural evolution from crystal precipitation from solution, the latter is referred to as primary nucleation whilst the former are secondary, ternary etc. nucleation processes. In principle, unlike the example of DL-norleucine shown here, the barrier to secondary nucleation (the solid-solid transformation) may be substantial, thus arresting the precipitate in a metastable form.

A common route to the production of relatively inert metastable polymorphs is to use alternative solvents. Whilst the basis for this is not well expressed in the literature, molecular simulations suggest that choice of solvent selects the polymorph on the basis of favorable surface-solvent interactions. However, this can only occur at the nucleation stage as surface-driven thermodynamic stabilization *ceases* with increasing crystal size. On the other hand, the barrier to secondary nucleation *increases* with crystal size. Hence, successful arresting of metastable polymorphs depends on an interplay of thermodynamic and kinetic aspects for which rationalization molecular scale insights are of crucial importance [154].

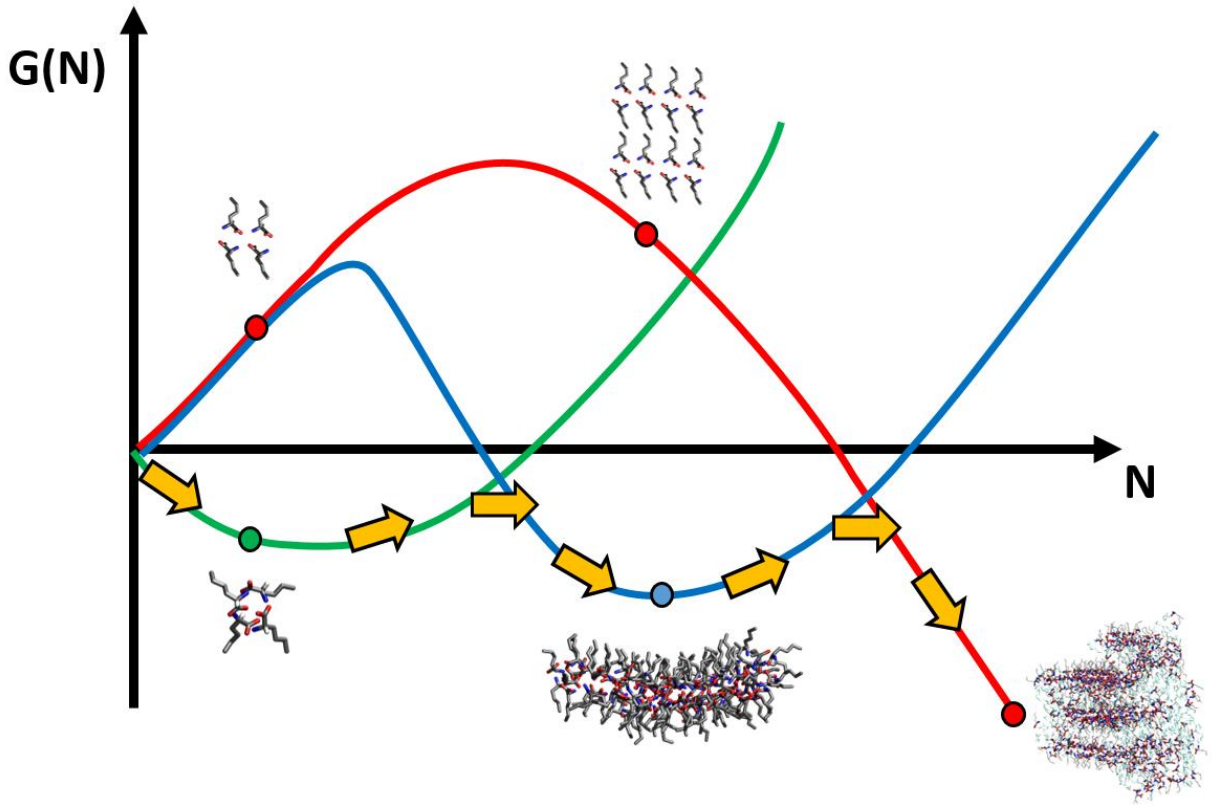

Figure 17. Illustration of size-induced polymorphic transitions as observed from molecular simulations of D/L-norleucine aggregation in a-polar solution. The least cost route to molecular crystal formation involves several structural transformations leading from micelles to bilayers to staggered bilayers and further ordering to reach the final crystal structure.

5.8 Kinetics from simulations

The primary kinetic parameters are the rate of nucleation and rate of interface advance at the selected temperature and pressure. Kinetics of nucleation are accessible from molecular simulation but studies to date have been on either nucleation from the melt or from solution. These simulations employ *directed* or *biased* methods e.g. umbrella sampling or metadynamics, wherein nucleation is coerced to occur whilst tracking the free energy [155-158]. This yields the free energy barrier to nucleation ΔG_N^*, which is the key quantity in the nucleation rate equation, Equation 19. Extending these methods to nucleation in a solid matrix (as in a solid-solid phase transformation) is feasible.

In contrast to the rate of nucleation, the rate of interface advance is readily obtainable from molecular simulation but requires the use of large systems. The initial step would be to induce the transformation using a biased/directed method to yield a molecular configuration comprising the emerging new phase embedded in the original phase with the phases separated by an interface. This configuration is then used as the initial state of a standard (brute force) molecular dynamics simulation. The rate of interface advance is tracked as a function of time as new layers deposit onto the growing new phase. Equating the deposition of the consecutive layers to length scale would yield the rate in unit length per unit time. There are many examples of estimates of rate of interface advance from molecular simulation, though most refer to crystal growth from either the melt or from solution [159-162]. Examples for solid-state phase transformations include DL-norleucine [127], and terephthalic acid [131].

6 Future perspectives

Our understanding of phase transitions in solids has developed via a number of distinct stages, beginning with empirical observations which were later enhanced with crystallographic structural data as a result of development and advances in diffraction methods. In the recent computing era, we have seen computer modelling employing simple physics-type models 'synthesising' a generic understanding of phase transitions. Subsequently, molecular simulations have drilled down to the molecular resolution and we are beginning to see the generic physics perspective of phase transitions being modulated by the rich behaviour of specific chemical species.

As we have shown, the macroscopic theoretical framework for the kinetics of crystal-crystal transformations is now pretty much resolved. Consequently, the expectation is to see (experimental) thermal kinetics studies of both nucleation and interface advance where the analysis includes the driving potential i.e. the extent of supercooling/superheating, rather than the use of the Arrhenius equation whose application may be inappropriate close to phase transition conditions. It is now feasible to go beyond the use a generalized kinetic equation such as the Avrami equation [80-82]. We can, in principle, numerically model crystal-crystal phase transformation kinetics using a coarse-grained, volume element representation (not molecular) wherein the sample crystal or crystals are sub-divided into small volume elements. The

transformation of each of the volume elements and the overall progression of the transformation is evolved using transition rates derived from experimental nucleation rates and anisotropic rates of interface advance. The modelling will include specification of the crystal morphology and size, and for polycrystalline samples a crystallite size distribution, for the particular material studied experimentally, thus matching its characteristics closely. For polycrystalline samples, this will enable the inclusion of a distribution of activation energies for nucleation [86], rather than a minimum or mean activation energy for nucleation that forms the basis of generalized kinetics equations. This numerical simulation approach would be more accurate, being more specific to the particular system and underpinned by experimentally-determined parameters.

Moving onto molecular simulations, as the review illustrates, this methodology has in the last two decades uncovered incomparable molecular insights, enhancing considerably our mechanistic understanding of phase transitions in crystals. Coupled to the insights is its powerful predictive capability e.g. crystal structure prediction and associated phase stability, and prediction of thermodynamics quantities such as lattice energies. How might the insights and the molecular-level mechanistic understanding contribute to chemical and pharmaceutical product development? The primary issue confronting industry is solid-state phase stability, in particular being able to identify *the stable polymorph*, and then, if chosen, to ensure its stability during manufacture and processing, e.g. granulation and compaction of tablets, and on storage. Deciding on the stable polymorph need not solve all stability issues: in principle, tableting could induce a phase transformation to a high-pressure form, which may or may not revert back to the stable form, and/or lead to undesired product characteristics or behavior such as tablet lamination. Beyond identifying the stable polymorph is the even more ambitious goal of exploiting the advantages of metastable polymorphs, such as higher solubility and dissolution rate, while ensuring their stability. The mechanistic insights from molecular simulations should enable the development for rational strategies for kinetically stabilizing metastable forms. A common approach for kinetic stabilization of metastable forms in ceramics, metals and alloys is the use of dopants i.e. the inclusion of a trace impurities into the lattice [163]. These third-party molecules inhibit the transformation. A similar approach in principle should work in molecular crystals. The knowledge of the key molecular interactions characterizing nucleation and interface advance could help to rationally design dopant molecules that inhibit nucleation and/or interface advance. Indeed, molecular simulation methods could be developed to screen such candidate

molecules before experimentation in the laboratory. The insightful design rules uncovered for crystal nucleation [164] and growth [165] could possibly map on to solid-state transformations. For instance, a potential dopant molecule should have both an affinity for the lattice and also be small enough to be sterically accommodated within the lattice.

Finally, we comment more broadly on the application of molecular simulation in industry, which is still very much in its infancy. We are acutely aware that whilst elegant simulation methods and approaches abound, many are developed in the context of simple models and/or exist in the form of bespoke computer codes that are not widely available or supported. This lack of capability for molecular systems, in particular pharmaceutical molecules, and the inaccessibility of the computer codes has limited wider uptake of molecular simulation. However, as evidenced by some of the literature reviewed here, a steadily increasing number of the molecular systems simulated are directly connected to application-driven research in the chemical and pharmaceutical industry. Further, there are important advances occurring in methodology including its implementation into robust codes. There is a focus on realistic models of pharmaceutical and biological molecules (in contrast to simplistic generic models) and an interest into modelling systems and processes that address challenges encountered not only in the wet lab, but also in pharmaceutical industry. This review is intended to provide such bridging - so, *how can application-driven problems such as polymorph control and stability in drug formulation benefit from molecular simulation?*

Our vision for the future is the routine use of molecular simulation in the workflow of the chemical and pharmaceutical industry in *real time*, informing fewer and better experiments, facilitating more effective products made efficiently, and time reduction to market. Indeed, molecular simulation is now an integral part of the predictive science strategy of a number of major pharmaceutical and chemical companies. BASF, for example, have recently committed to installing a high-performance supercomputing facility with stated applications being a better understanding of catalyst surfaces and faster design of new polymers.

The predictive capability of molecular simulation will drive screening of polymorphic forms in tandem with experimental programmes. The routine ability to predict the crystal structure from a 2-D molecular structure would open the door to predicting solid state properties such as dissolution rate, solubility, crystal surface energy, and mechanical properties without having to

synthesise the molecule, setting the foundations for in-silico drug development. This will also give rise to commercial opportunity by providing a list of possible (energetically reasonably favorable) candidates, hence expanding the realm of targetable polymorph structures. Beyond crystalline phase stability and polymorphic transitions, molecular simulation can be used to investigate a wide spectrum of systems in all the main states of matter: solid, soft matter, liquid and solution, and gas phase. Solution and liquid state systems are wholly accessible to standard molecular simulation, as are soft matter systems such as simple lipid membranes (see for instance [166] that can enable the prediction of permeation across membranes [167]. Thus, how drugs interact with cyclodextrins or polymer nanoparticles in solution, micellar systems [168], nanoemulsions, and membrane permeation can be investigated in a routine manner. There are still some technical challenges with respect to simulating the more condensed phases (e.g. structural organisation in the essentially crystalline lipid phases of the skin), simulation of longer time scale phenomena (e.g. precipitation of solids from solution), and the simulation of large scale systems e.g. monoclonal antibodies. However, methods for resolving these issues are in place though need to be extended to realistic systems and/or implemented in accessible and robust computer codes. Indeed, it is now timely to consider applications of molecular simulation within the workflow of the industry. Molecular simulation expertise needs to be integrated into the industrial project teams, where it can add value in real time (that is on scales of hours to weeks, rather than months and years).

While the broad capability of molecular simulation demonstrates its readiness to not only supporting drug design but also its formulation, we are still at the beginning of exploiting the full scope of this emerging technique. Simulation methodology not only needs further development (we attempted to describe the status-quo, but are well aware that method development will probably never actually end), but also requires maturing in terms of ready modelling of realistic molecular systems, industry standard computer codes implementing advanced methods, user-friendliness, and faster turnaround of simulation results. For all of these aspects, we feel that current progress and future perspectives are indeed appealing: modelling packages are increasingly becoming more accurate, faster and easier to use. The software advances are flanked by the ongoing improvement of CPUs and the increasing application of GPUs (graphics processors) which have drastically reduced hardware costs whilst increasing process capacity. The latter issue is not a purely economic point, but also allows the scope of model complexity to

increase continuously. Thus, we are able to simulate increasingly larger molecular systems, both increase in the complexity of individual molecules and also the number of molecules in the system. Moreover, large-scale computation parallelization offers screening of a variety of compositions and process conditions within reasonable time scales.

All this makes molecular simulations an increasingly indispensible approach to pharmaceutical development. Within the next decade, we feel that the role of molecular simulation in drug formulation will become very similar to the role of computational modelling in drug design. While fast and approximate models provide quick screening of candidates, more dedicated molecular simulations will elaborate in-depth understanding to drive innovation beyond trial-and-error. Along these lines, the gaps between experimental and computational characterization are decreasing and modern innovation will surely rely on both.

References

[1] M. Murakami1, K. Hirose, K. Kawamura, N. Sata, Y. Ohishi, Post-perovskite phase transition in MgSiO3, Science 304 (2004) 855-858.

[2] F. J. Manjon, D. Errandonea, Pressure-induced structural phase transitions in materials and earth sciences, Physica Status Solidi B - Basic Solid State 246 (2009) 9-31.

[3] R. E. Newnham, Phase transformations in smart materials, Acta Cryst. A 54 (1998) 729-737.

[4] G. Kostorz, Phase transformations in materials, Ed., Wiley-VCH Verlag GmbH, 2001.

[5] B. Fultz, Phase Transitions in Materials, 1st Edition, Cambridge University Press, 2014.

[6] A. M. Belcher, X. H. Wu, R. J. Christensen, P. K. Hansma, G. D. Stucky, D. E. Morse, Control of crystal phase switching and orientation by soluble mollusc-shell proteins, Nature 381 (1996) 56.

[7] S. V. Dorozhkin, M. Epple, Biological and medical significance of calcium phosphates, Angew. Chem., Int. Ed. 41 (2002) 3130.

[8] Y. H. Tseng, C. Y. Mou, J. C. C. Chan, Solid-state NMR study of the transformation of octacalcium phosphate to hydroxyapatite: A mechanistic model for central dark line formation, J. Am. Chem. Soc. 128 (2006) 6909.

[9] M. Ghosh, S. Banerjee, M. A. S. Khan, N. Sikdera, A. K. Sikder, Understanding metastable phase transformation during crystallization of RDX, HMX and CL-20: experimental and DFT studies, Phys. Chem. Chem. Phys. 18 (2016) 23554.

[10] K. R. Morris, U. J. Griesser, C. J. Eckhardt, J. G. Stowell, Theoretical approaches to physical transformations of active pharmaceutical ingredients during manufacturing processes, Advanced Drug Delivery Reviews 48 (2001) 91–114.

[11] G. G. Z. Zhang, D. Law, E. A. Schmitt, Y. H. Qiu, Phase transformation considerations during process development and manufacture of solid oral dosage forms, Advanced Drug Delivery Reviews, 56 (2004) 371-390.

[12] J. K. Haleblian, W. McCrone, Pharmaceutical applications of polymorphism, J. Pharm. Sci. 58 (1969) 911-929.

[13] J. K. Haleblian, Characterization of habits and crystalline modification of solids and their pharmaceutical applications, J. Pharm. Sci. 64 (1975) 1269-1288.

[14] S. R. Vippagunta, H. G. Brittain, D. J. W. Grant, Crystalline solids, Advanced Drug Delivery Reviews 48 (2001) 3-26.

[15] J. Bernstein, Polymorphism in Molecular Crystals; Oxford University Press: Oxford, U.K., 2002.

[16] C. R. Gardner, C. T. Walsh, O. Almarsson, Drugs as materials: valuing physical form in drug discovery, Nature Reviews Drug Discovery 3 (2004) 926-934.

[17] J. Bernstein, Polymorphism - A Perspective, Crystal Growth & Design (2011) 11, 632-650.

[18] J. Bauer, S. Spanton, R. Henry, J. Quick, W. Dziki, W. Porter, J. Morris, Ritonavir crystal forms - an extraordinary example of conformational polymorphism, Pharmaceutical Research 18 (2001) 859-866.

[19] ANDAs: Pharmaceutical Solid Polymorphism, Chemistry, Manufacturing, and Controls Information, FDA Guidance for Industry, July 2007,

[20] International Conference on Harmonisation (ICH) Q6A. Specifications: Test procedures and acceptance criteria for new drug substances and new drug products: chemical Substances, Step 4, October 1999.

[21] M. P. Allen, D. J. Tildesley, Computer Simulation Of Liquids, Oxford Science Publications, 2006.

[22] D. Frenkel, B. Smit, Understanding Molecular Simulation: From Algorithms to Applications, 2nd Edition, Academic Press, 2001.

[23] D. P. Landau, K. Binder, A guide to Monte Carlo simulations in statistical physics, 3rd Edition, Cambridge University Press, 2009.

[24] J. W. Christian, The theory of transformations in metals and alloys, Part I, Equilibrium and general kinetic theory, 2nd Ed. Oxford: Pergamon, 1975.

[25] C. N. R Rao, K. J. Rao, Phase Transitions in Solids, McGraw Hill, N.Y., 1978.

[26] P. Toledano, V. Dmitriev, Reconstructive phase transitions (in crystals and quasicrystals), Singapore: World Scientific, 1996.

[27] Y. V. Mnyukh, Fundamentals of solid-state phase transitions, ferromagnetism and ferroelectricity; Authorhouse: Bloomington, IN, 2001.

[28] F. H. Herbstein, On the mechanism of some first-order enantiotropic solid-state phase transitions: from Simon through Ubbelohde to Mnyukh, Acta Cryst. B62 (2006) 341-383.

[29] R. D. James, K. F. Hane, Martensitic transformations and shape memory materials, Acta Materials 48 (2000) 197-222.

[30] M. T. Dove, Theory of displacive phase transitions in minerals, American Mineralogist 82 (1997) 213-244.

[31] A. R. Ubbelohde, Crystallography and the phase rule, Brit. J. Appl. Phys. 7 (1956) 313-321.

[32] A. R. Ubbelohde, Thermal transformation in solids, Quart. Rev. London 11 (1957) 246-272.

[33] A. R. Ubbelohde, Transitions between condensed phases of matter (second Van't Hoff lecture), Kon. Ned. Akad. Wetens. Proc. 65 B (1962) 459-471.

[34] A. R. Ubbelohde, Premonitory phenomena in phase transitions in solids, Z. Phys. Chem. N. F. 37 (1963) 183-195.

[35] A. R. Ubbelohde, Molecular movements and phase transitions in solids. 1 – Thermodynamic and structural aspects of phase transitions that are wholly or partly continuous, J. Chim. Phys. 62 (1966) 33-42.

[36] A. J. Cruz-Cabeza, J. Bernstein, Conformational Polymorphism, Chemical Reviews 114, (2014) 2170-2191.

[37] A. Y. Lee, D. Erdemir, A. S. Myerson, Crystal polymorphism in chemical process development, Annu. Rev. Chem. Biomol. Eng. 2 (2011) 259–80.

[38] A. J. Cruz-Cabeza, S. M. Reutzel-Edens; Joel Bernstein, Facts and fictions about polymorphism, Chem. Soc. Rev., 2015, 44, 8619

[39] S.R. Byrn, R.R. Pfeiffer, J.G. Stowell, Solid-State Chemistry of Drugs, SSCI, West Lafayette, IN, 1999.

[40] H.G. Brittain, E.F. Fiese, Effects of pharmaceutical processing on drug polymorphs and solvates, in: H.G. Brittain (Ed.), Polymorphism in Pharmaceutical Solids, Vol. 95, Dekker, New York, 1999, pp. 331–361.

[41] H. G. Ibrahim, F. Pisano, A. Bruno, Polymorphism of phenylbutazone: Properties and compressional behavior of crystals, J. Pharm. Sci. 66 (1977) 669-673.

[42] H. K. Chan, E. Doelker, Polymorphic transformation of some drugs under compression, Drug Dev. Ind. Pharm. 11 (1985) 315-332.

[43] F. P. A. Fabbiani, D. R. Allan, W. I. F. David, A. J. Davidson, A. R. Lennie, S. Parsons, C. R. Pulham, J. E. Warren, High-pressure studies of pharmaceuticals: An exploration of the behavior of piracetam, Crystal Growth & Design, 7 (2007) 1115-1124.

[44] H. G. Brittain, Effects of mechanical processing on phase composition. J. Pharm. Sci. 91 (2002)1573–80.

[45] A. Findlay (1951) The Phase rule and its Applications, 9th Ed. Dover N.Y.

[46] P. W. Bridgman, A transition of silver oxide under pressure, Rec. Trav. Chim. (1932) 51, 627-632.

[47] A. J. Dornell, W. A. McCollum, High Temp. Sci. 2 (1970) 331.

[48] O. Lehmann, Ueber physikalische untersuchungen, Z. Kristallographia. 1 (1877) 97-131.

[49] O. Lehmann, in Molekularphysik, Ed. W. Engelmann, Leipzig, 1888.

[50] A. R. Ehrenfest, Phase transitions in the usual and generalized sense, classified according to the singularities of the thermodynamic potential, Leiden Comm. Suppl. No. 75b (1933).

[51] M. J. Buerger, in Phase Transformations in Solids, Ed. R. Smoluchowski, J. E. Mayer, W. A. Weyl, John Wiley and Son, N.Y., 1951.

[52] M. J. Buerger, Polymorphism and phase transformations, Fortschr. Mineral 39 (1961) 9-24.

[53] M. J. Buerger, Phase transformations, Soviet Physics Crystallography USSR 16 (1972) 959.

[54] K. Otsuka, C. M. Wayman, Eds. Shape Memory Materials; Cambridge University Press: Cambridge, 1998.

[55] P. M. Kelly, L. R. F. Rose, The martensitic transformation in ceramics - its role in transformation toughening, Prog. Materials Sci. 2002, 47, 463-557.

[56] Y. V. Mnyukh, N. A. Panfilova, N. N. Petropavlov, N. S. Uchvatova, Polymorphic transitions in molecular crystals. 3. Transitions exhibiting unusual behaviour, J. Phys. Chem. Solids 36 (1975) 127-144.

[57] P. Naumov, S. Chizhik, M. K. Panda, N. K. Nath, E. Boldyreva, Mechanically Responsive Molecular Crystals, Chem. Rev. 115 (2015) 12440−12490.

[58] Eyring et al. J. Chem Phys. 3 (1935) 786.

[59] D. Zahn, Modeling martensitic transformations in crystalline solids: validity and redesign of geometric approaches, Z. Krist. 226 (2011) 568-575.

[60] D. Zahn, H. Tlatlik, Atomistic in-situ investigation of the morphogenesis of grains during pressure-induced phase transitions: molecular dynamics simulations of the *B1-B2* transformation of RbCl, Chem. Eur. J. 16 (2010) 13385-13389.

[61] Y. V. Mnyukh, A. I. Kitaigorodskiy, Y. G. Asadov, A study of the polymorphic transition in monocrystalline para-dicholorobenzene, Zh. Eksp. Teor. Fiz. 48 (1965) 19 (Soviet Physics -JETP 21 (1965) 12).

[62] Y. V. Mnyukh, N. I. Musaev, A. I. Kitaigorodskiy, Crystal Growth upon polymorphous transformation in glutaric acid and hexachlorotane, Akad. Nauk. SSSR 174 (1967) 345 (Soviet Physics -Doklady 12 (1967) 409).

[63] Y. V. Mnyukh, Molecular mechanism of polymorphic transitions, Dokl. Akad. Nauk. SSSR 201 (1971) 573-576 (Soviet Physics -Doklady 16, 977-980).

[64] Y. V. Mnyukh, N. N. Petropavlov, Polymorphic transitions in molecular crystals. 1. Orientations of lattices and interfaces, J. Phys. Chem. Solids 33 (1972) 2079-2087.

[65] Y. V. Mnyukh, N. A. Panfilova, Polymorphic transitions in molecular crystals. 2. Mechanism of molecular re-arrangement at the contact surface, J. Phys. Chem. Solids 34 (1973) 159-170.

[66] Y. V. Mnyukh, Polymorphic transitions in crystals – kinetics, Mol. Cryst. Liq. Cryst. 52 (1979) 505-521.

[67] D. Turnbull, in Solid State Physics, Vol. 3, Ed. F. Seitz, D. Turnbull, Academic Press, N.Y., 1956.

[68] M. Volmer, A. Weber, Z. Phys. Chem. 119 (1925) 277.

[69] R. Becker, W. Doring, Kinetische behandlung der keimbildung in übersättigten dämpfen, Ann. Phys. (1935) 24, 719.

[70] N. H. Hartshorne, P. M. Swift, Studies in polymorphism. Part VII. The linear rate of polymorphic transformation of cubic to monoclinic carbon tetrabromide, J. Chem. Soc. (1955) 3705-3720.

[71] N. H. Hartshorne, M. Thackray, Studies in polymorphism. Part VIII. The linear rate of transformation of β- into α-sulphur at low temperatures and at temperatures just below the transition point, J. Chem. Soc. (1957) 2122.

[72] R. S. Bradley, The energetics and statistical mechanics of the kinetics of solid-->solid reactions, J. Phys. Chem. (1956) 60, 1347-1354.

[73] S. E. Boulfelfel, D. Zahn, O. Hochrein, Y. Grin, S. Leoni, Low-dimensional sublattice melting by pressure: superionic conduction in the phase interfaces of the fluorite-to-cotunnite transition of CaF2, Phys. Rev. B. (2006) 74, 94106.

[74] J. Anwar, P. Barnes, S.M. Clark, E. Dooryhee, D. Hausermann, S.E. Tarling, The use of fast powder diffraction methods to study transformations, J. Material Science Letters 9 (1990) 436-439.

[75] D. A. Young, Decomposition of Solids, Pergamon Press, Oxford, 1966.

[76] Y. Kishi, M. Matsuoka, Phenomena and kinetics of solid state polymorphic transition of caffeine, Crystal Growth & Design, 10 (2010) 2916-2920.

[77] M. E. Villafuerte-Castrajon, A. R. West, Kinetics of polymorphic transitions in tetrahedral structures. Part 1. - Experimental methods and the transition $\gamma \rightarrow \beta$ Li_2ZnSiO_4, J. Chem. Soc. Farad. 1 75 (1979) 374-384.

[78] M. E. Villafuerte-Castrajon, A. R. West, Kinetics of polymorphic transitions in tetrahedral structures. Part 2. - Temperature dependence of the transition $\beta \rightleftharpoons \gamma$ Li_2ZnSiO_4, J. Chem. Soc. Farad. 1 77 (1981) 2297-2307.

[79] D. Zahn, Nucleation mechanism and kinetics of the perovskite to post-perovskite transition of MgSiO3 under extreme conditions, Chem. Phys. Lett. 573 (2013) 5-7.

[80] M. J. Avrami, Kinetics of phase change. I General theory, Chem. Phys. (1939) 7, 1103.

[81] M. J. Avrami, Kinetics of phase change. II Transformation-time relations for random distribution of nuclei, Chem. Phys. (1940) 8, 212.

[82] M. J. Avrami, Granulation, phase change, and microstructure kinetics of phase change. III, Chem. Phys. (1941) 9, 177.

[83] W. A. Johnson, R. F. Mehl, Reaction kinetics in processes of nucleation and growth, Metallurgical and Materials Trans. B AIME 135 (1939) 416-458.

[84] B. V. Erofeyev, A generalized equation of chemical kinetics and its application in reactions involving solids, C. R. Dokl. Akad. Sci. URSS 52 (1946) 511-514.

[85] R. E. Cech, D. Turnbull, Hetrogeneous nucleation of the martensite transformation, AIME Trans., 206 (1956) 124-132.

[86] A. K. Sheridan, J. Anwar, Kinetics of the solid-state phase transformation of form β to γ of sulfanilamide using time-resolved energy-dispersive x-ray diffraction, Chem. Mater. 8 (1996) 1042.

[87] P. T. Cardew, R. J. Davey, A. J. Ruddick, Kinetics of polymorphic solid-state transformations, J. Chem. Soc. Farad. Trans. 2 Molecular & Chemical Physics 80 (1984) 659-668.

[88] C. L. Magee, The kinetics of martensite formation in small particles, Metallurgical Trans. 2 (1971) 2419-2430.

[89] W. Christian, Computer Program: Ising 3D checkerboard decomposition model,Version 1.0 (2013), WWW Document http://www.compadre.org/Repository/document/ServeFile.cfm?ID=13033&DocID=3602.

[90] L. Monticelli, D. P. Tieleman, Force fields for classical molecular dynamics, in Methods in Molecular Biology, Clifton, N.J., 2013, pp 197-213.

[91] A. D. Mackerell Jr, Empirical Force Fields for Biological Macromolecules: Overview and Issues, Journal of Computational Chemistry 25 (2004) 1584–1604.

[92] M. A. Neumann, F. J. J. Leusen, J. Kendrick, A major advance in crystal structure prediction, Angew. Chem. Int. Ed. 47 (2008) 2427–2430.

[93] M. A. Neumann, Tailor-made force fields for crystal-structure prediction, J. Phys. Chem. B 112 (2008) 9810–9829.

[94] A. M. Reilly et al Report on the sixth blind test of organic crystal structure prediction methods, Acta Cryst B: Structural Sciences and Crystal Engineering Materials 72 (2016) 439-459.

[95] M. Parrinello, A. Rahman, Crystal structure and pair potentials: a molecular-dynamics Study, Phys. Rev. Lett. 45 (1980) 1196-1199.

[96] M. Parrinello, A. Rahman, Polymorphic transitions in single crystals: A new molecular dynamics method, Journal of Applied Physics 52 (1981) 7182.

[97] A. Laio, M. Parrinello, Escaping free energy minima, Proc Natl Acad Sci USA 99 (2002) 12562–12566.

[98] A. Barducci, M. Bonomi, M. Parrinello, Metadynamics, Wires Computational Molecular Science 1 (2011) 826-843.

[99] R. Martonak, A. Liao, M. Parrinello, Predicting Crystal Structures: The Parrinello-Rahman method revisited, Physical Review Letters 90 (2003) 075503.

[100] A. B. Belonoshko, S. Arapan, R. Martonak, A. Rosengren, MgO phase diagram from first principles in a wide pressure-temperature range, Physical Review B 81 (2010), 054110.

[101] R. Martonak, A. Laio, M. Bernasconi, C. Ceriani, P. Raiteri, F. Zipoli, M. Parrinello, Simulation of structural phase transitions by metadynamics, Zeitschrift für Kristallographie-Crystalline Materials 220 (2005) 489-498.

[102] A. R. Oganov, R. Martonak, A. Laio, P. Raiteri, M. Parrinello, Anisotropy of Earth's D layer and stacking faults in the MgSiO3 post-perovskite phase, Nature 438 (2005) 1142-1144.

[103] P. G. Bolhuis, D. Chandler, C. Dellago, P. L. Geissler, Transition path sampling: throwing ropes over rough mountain passes, in the dark, Annual Review Phys. Chem. 53 (2002) 291-318.

[104] B. Peters, Recent advances in transition path sampling: accurate reaction coordinates, likelihood maximisation and diffusive barrier-crossing dynamics, Molecular Simulation 36 (2010) 1265-1281.

[105] D. Zahn and S. Leoni, Nucleation and Growth in Pressure-Induced Phase Transitions from Molecular Dynamics Simulations: Mechanism of the Reconstructive Transformation of NaCl to the CsCl-type structure, Phys. Rev. Lett. 92 (2004), 250201-04.

[106] S.M. Woodley and R. Catlow (2008) Crystal structure prediction from first principles, Nature Materials 7 (2008) 937-946.

[107] A. Gavezzotti, Are crystal structures predictable? Acc. Chem. Res. 27 (1994) 309-314.

[108] T.S. Thakur, R. Dubey, G.R. Desiraju, Crystal structure prediction, Ann. Rev. Physical Chemistry 66 (2015) 21-42.

[109] S. L. Price, M. Leslie, G. W. A. Welch, M. Habgood, L. S. Price, P. G. Karamertzanis, G. M. Day, Modelling organic crystal structures using distributed multipole and polarizability-based model intermolecular potentials, Phys. Chem. Chem. Phys. 12 (2010) 8478–8490.

[110] J. Nyman, G. M. Day, Static and lattice vibrational energy differences between polymorphs. Crystengcomm 17 (2015) 5154-5165

[111] S. C. Tuble, J. Anwar, J. D. Gale, An approach to developing a force field for molecular simulation of martensitic phase transitions between phases with subtle differences in energy and structure, J. Am. Chem. Soc. 126 (2004) 396-405.

[112] J. Chatchawalsaisin, J. Kendrick, S. C. Tuble, J. Anwar, An optimized force field for crystalline phases of resorcinol, CrystEngComm, 10 (2008) 437–445.

[113] H. de Waard, A. Amani, J. Kendrick, W. L. J. Hinrichs, H. W. Frijlink, J. Anwar, Evaluation and optimization of a force field for crystalline forms of mannitol and sorbitol, J. Phys. Chem. B, 114 (2010) 429-436.

[114] N. L. Allan, D. Gustavo, D. Barrera, J. A. Purton, C. E. Simsa, M. B. Taylor, Ionic solids at elevated temperatures and/or high pressures: lattice dynamics, molecular dynamics, Monte Carlo and ab initio studies, Phys. Chem. Chem. Phys. 2 (2000) 1099-1111.

[115] D. Frenkel, A. J. C. Ladd, New Monte Carlo method to compute the free energy of arbitrary solids. Application to the fcc and hcp phases of hard spheres, Journal of Chemical Physics 81 (1984) 3188-3193.

[116] J. Anwar, D. Frenkel, M. G. Noro, Calculation of the melting point of NaCl by molecular simulation, Journal of Chemical Physics 118 (2003) 728-735.

[117] D. A. Kofke, Gibbs-Duhem integration: a new method for direct evaluation of phase coexistence by molecular simulation, Molecular Physics 78 (1993) 1331-1336.

[118] S. Singh, M. Chopra, J. J. de Pablo, Density of states–based molecular simulations, Annual Review of Chemical and Biomolecular Engineering 3 (2012) 369-394.

[119] W. C. Mackrodt, E.-A. Williamson, D. Williams, N. L. Allan, A first-principles Hartree-Fock description of MnO at high pressures, Phil. Mag. B 77 (1998) 1063-1075.

[120] R. E. Westacott, P. M. Rodger, Full-coordinate free-energy minimisation for complex molecular crystals: type I hydrates, Chemical Physics Letters, 262 (1996) 47-51.

[121] E. Sanz, C. Vega, J. L. F. Abascal, L. G. MacDowell, Phase diagram of water from computer simulation, Phys. Rev. Lett. 92 (2004) 255701.

[122] G. S. Pawley, G. W. Thomas, Computer Simulation of the Plastic-to-Crystalline Phase Transition in SF_6, Physical Review Letters 48 (1982) 410-413.

[123] K. Refson, S. Pawley Molecular dynamics studies of the condensed phases of n-butane and their transitions I. Techniques and model results, Molecular Physics, 61 (1986b) 669-692.

[124] K. Refson, S. Pawley, Molecular dynamics studies of the condensed phases of n-butane and their transitions II. The transition to the true plastic phase, Molecular Physics 61 (1986a) 693-709.

[125] G. B. Olson and H. Hartman, Martensite and life: displacive transformation as biological processes, J. Phys. Paris, Colloq. 43 (1982) C4-855 - C4-865.

[126] W. Falk, R. D. James, Elasticity theory for self-assembled protein lattices with application to the martensitic phase transition in bacteriophage T4 tail sheath, Physical Review E 73 (2006) 011917.

[127] J. Anwar, S. C. Tuble, J. Kendrick, Concerted molecular displacements in a thermally-induced solid-state transformation in crystals of DL-norleucine, J. Am. Chem. Soc. (2007) 129, 2542-2547.

[128] D. Zahn, J. Anwar, Size-dependent phase stability of a molecular nanocrystal: a proxy for investigating the early stages of crystallization, Chem Euro. J. 17 (2011) 11186-11192.

[129] D. Zahn, J. Anwar, Collective displacements in a molecular crystal polymorphic transformation, RSC Advances 3 (2013) 12810–12815.

[130] J. van den Ende, B. Ensing, H. Cuppen, Energy barriers and mechanisms in solid-solid polymorphic transitions exhibiting cooperative motion. Crystengcomm 18 (2016) 4420-4430.]

[131] G. T. Beckham, B. Peters, C. Starbuck, N. Variankaval, B. L. Trout, Surface-mediated nucleation in the solid-state polymorph transformation of terephthalic acid, J. Am. Chem. Soc. (2007) 129, 4714–4723.

[132] R. J. Davey, S. J. Maginn, S. J. Andrews, A. M. Buckley, D. Cottier, P. Dempsey, J. E. Rout, D. R. Stanley, A. Taylor, Morphology and polymorphism in molecular crystals : terephthalic acid, J. Chem. Soc. Faraday Trans. 90 (1994) 1003-1009.

[133] D. Zahn, O. Hochrein, S. Leoni, Multicenter multidomain B1-B2 pressure-induced reconstructive phase transition in potassium fluoride, Physical Review B 72 (2005) 094106.

[134] D. Zahn, Y. Grin, S. Leoni, The mechanism of the pressure-induced wurtzite to rocksalt transition of cadmium selenide, Physical Review B 72 (2005) 064110-17.

[135] S. Scandolo, M. Bernasconi, G. L. Chiarotti, P. Focher, E. Tosatti, Pressure-induced transformation path of graphite to diamond. Phys. Rev. Lett. 74 (1995) 4015-4018.

[136] S. E. Boulfelfel, D. Zahn, Y. Grin, S. Leoni, Walking the path from B4 to B1 type structures in GaN, Physical Review Letters 99 (2007) 125505.

[137] S. Devani, J. Anwar, A molecular dynamics simulation study of the effects of defects on the transformation pressure of polymorphic phase transformations, J. Chem. Phys. 105 (1996) 3215-3218.

[138] H. Z. Zhang, J. F. Banfield, Thermodynamic analysis of phase stability of nanocrystalline titania, J. Materials Chemistry 8 (1998) 2073-2076.

[139] M. R. Ranade, A. Navrotsky, H. Z. Zhang, J. F. Banfield, S. H. Elder, A. Zaban, P. H. Borse, S. K. Kulkarni, G. S. Doran, H. J. Whitfield, Energetics of nanocrystalline TiO2, Proc. Natl. Acad.Sci. U.S.A. 99 (2002) 6476-6481.

[140] A. A. Levchenko, G. Li, J. Boerio-Goates, B. F. Woodfield, A. Navrotsky, TiO2 stability landscape: polymorphism, surface energy, and bound water energetics, Chem. Mater. 18 (2006) 6324-6332.

[141] M. W. Pitcher, S. V. Ushakov, A. Navrotsky, B. F. Woodfield, G. Li, J. Boerio-Goates, B. M. Tissue, Energy crossovers in nanocrystalline zirconia, J. Am. Ceram. Soc. 88 (2005) 160-167.

[142] J. M. McHale, A. Auroux, A. J. Perrotta, A. Navrotsky, Surface energies and thermodynamic phase stability in nanocrystalline aluminas, Science 277 (1997) 788-791.

[143] C. Wang, J. Chen, G. Yang, N. Xu, Thermodynamic stability and ultrasmall-size effect of nanodiamonds, Angewandte Chemie Int Ed. 44 (2005) 7414–7418.

[144] S. Blonski, S. H. Garofalini, Molecular dynamics simulations of α-alumina and γ-alumina surfaces, Surf. Sci. 295 (1993) 263.

[145] R. B. Hammond, K. Pencheva, K. J. Roberts, Simulation of energetic stability of facetted L-glutamic acid nanocrystalline clusters in relation to their polymorphic phase stability as a function of crystal size, J. Physical Chemistry B 109 (2005) 19550-19552.

[146] Q. Jiang, W. D. Ward, Crystallisation under nanoscale confinement, Chem. Soc. Rev. 43 (2014) 2066-2079.

[147] B. D. Hamilton, M. A. Hillmyer, M. D. Ward, Glycine polymorphism in nanoscale crystallization chambers, Crystal Growth & Design 8 (2008) 3368-3375.

[148] G. T. Rengarajan, D. Enke, M. Steinhart, M. Beiner, Size-dependent growth of polymorphs in nanopores and Ostwald's step rule of stages, Phys. Chem. Chem. Phys.13 (2011) 21367–21374.

[149] J. M. Ha, J. H. Wolf, M. A. Hillmyer, M. D. Ward, Polymorph selectivity under nanoscopic confinement J. Am. Chem. Soc.,126 (2004) 3382–3383.

[150] A. M. Belenguer; G. I. Lampronti; A. J. Cruz-Cabeza; C. A. Hunter; J. K. M. Sanders, Solvation and surface effects on polymorph stabilities at the nanoscale, Chem. Sci., 2016, 7, 6617

[151] P. Ectors, P. Duchstein, D. Zahn, From oligomers towards a racemic crystal: molecular simulation of DL-norleucine crystal nucleation from solution, CrystEngComm,17 (2015) 6884-6889.

[152] W. Ostwald, Studien über die Bildung und Umwandlung fester Körper, Z. Phys. Chem. 1897, 22, 289 – 330.

[153] N. I. Stranski, D. Totomanow, Rate of formation of (crystal) nuclei and the Ostwald step rule. Z. Phys. Chem. 163 (1933) 399-408.

[154] D. Zahn, Thermodynamics and kinetics of prenucleation clusters, classical and non-classical nucleation, Chem. Phys. Chem.16 (2015) 2069-2075.

[155] C. Valeriani, E. Sanz, D. Frenkel, Rate of homogeneous crystal nucleation in molten NaCl, J. Chem. Phys. 2005, 122, 194501.

[156] A. Brukhno, J. Anwar, R. Davidchack, R. Handel, Challenges in molecular simulation of homogeneous ice nucleation, Journal of Physics: Condensed Matter 20 (2008) 1-17.

[157] M. Salvalaglio, C. Perego, F. Giberti, M. Mazzottia, M. Parrinello, Molecular-dynamics simulations of urea nucleation from aqueous solution, Proc. National Acad. Sciences 112 (2014) E6-E14.

[158] J. Anwar, D. Zahn, Uncovering molecular processes in crystal nucleation and growth by using molecular simulation, Angew. Chem. Int. Ed. 50 (2011) 1996 – 2013.

[159] P. Ectors, W. Sae-Tang, J. Chatchawalsaisin, D. Zahn, J. Anwar, The molecular mechanism of α-resorcinol's asymmetric crystal growth from the melt, Cryst. Growth Des. 15 (2015) 4026-4031.

[160] P. Ectors, J. Anwar, D. Zahn, Two-step nucleation rather than self-poisoning: An unexpected mechanism of asymmetrical molecular crystal growth, Cryst. Growth Des. 15 (2015) 5118−5123.

[161] S. Piana, M. Reyhani, J. D. Gale, Simulating micrometre-scale crystal growth from solution, Nature 438 (2005) 70-73.

[162] M. Salvalaglio, T. Vetter, F. Giberti, M. Mazzotti, M. Parrinello, Uncovering molecular details of urea crystal growth in the presence of additives, J. Am. Chem. Soc., 134 (2012) 17221–17233.

[163] B. Djuricic, S. Pickering, P. Glaude, D. McGarry, P. Tambuyser, Thermal stability of transition phases in zirconia-doped alumina, J. Material Science 21 (1997) 589-601.

[164] J. Anwar, P. K. Boateng, R. Tamaki, S. Odedra, Mode of action and design rules for additives that modulate crystal nucleation, Angewandte Chemie Int Ed. 48 (2009) 1596–1600.

[165] M. Lahav and L. Leiserowitz, Tailor-made auxiliaries for the control of nucleation, growth and dissolution of two- and three-dimensional crystals, Journal of Physics D: Applied Physics, 26 (1993) B22-B31.

[166] R. Notman, J. Anwar, Breaching the skin barrier - insights from molecular simulation of model membranes, Advanced Drug Delivery Reviews 65 (2013) 237–250.

[167] D. Bemporad, J.W. Essex, C. Luttmann, Permeation of small molecules through a lipid bilayer: a computer simulation study, J. Phys. Chem. B 108 (2004) 4875–4884.

[168] A. Amani, P. York, H. de Waard, J. Anwar, Molecular dynamics simulation of a polysorbate 80 micelle in water, Soft Matter, 7 (2011) 2900-2908.